REPORT DOCUMENTATION PAGE	Form Approved OMB No. 0704-0188

1. AGENCY USE ONLY *(Leave blank)*	2. REPORT DATE	3. REPORT TYPE AND DATES COVERED
	7 Jan 99	THESIS

4. TITLE AND SUBTITLE
PREDICTING EAST COAST SEA BREEZE INITIATED CONVECTION NEAR CAPE CANAVERAL, FLORIDA

5. FUNDING NUMBERS

6. AUTHOR(S)
CAPT KELLY JONATHAN L

7. PERFORMING ORGANIZATION NAME(S) AND ADDRESS(ES)
FLORIDA STATE UNIVERSITY

8. PERFORMING ORGANIZATION REPORT NUMBER

9. SPONSORING/MONITORING AGENCY NAME(S) AND ADDRESS(ES)
THE DEPARTMENT OF THE AIR FORCE
AFIT/CIA, BLDG 125
2950 P STREET
WPAFB OH 45433

10. SPONSORING/MONITORING AGENCY REPORT NUMBER
FY99-20

11. SUPPLEMENTARY NOTES

12a. DISTRIBUTION AVAILABILITY STATEMENT
Unlimited distribution
In Accordance With AFI 35-205/AFIT Sup 1

12b. DISTRIBUTION CODE

13. ABSTRACT *(Maximum 200 words)*

14. SUBJECT TERMS	15. NUMBER OF PAGES 49
	16. PRICE CODE

17. SECURITY CLASSIFICATION OF REPORT	18. SECURITY CLASSIFICATION OF THIS PAGE	19. SECURITY CLASSIFICATION OF ABSTRACT	20. LIMITATION OF ABSTRACT

THE FLORIDA STATE UNIVERSITY

COLLEGE OF ARTS AND SCIENCES

PREDICTING EAST COAST SEA BREEZE INITIATED CONVECTION NEAR CAPE CANAVERAL, FLORIDA

By

JONATHAN LEE KELLY

A thesis submitted to the
Department of Meteorology
in partial fulfillment of the
requirements for the degree of
Master of Science

Degree Awarded:

Summer Semester, 1998

The members of the Committee approve the thesis of Jonathan L. Kelly defended on July 9, 1997.

Henry E. Fuelberg
Professor Directing Thesis

Kevin A. Kloesel
Committee Member

James J. O'Brien
Committee Member

ACKNOWLEDGEMENTS

This research was funded by the Air Force Weather Agency (AFWA) from sub-award S96-75662 to Florida State University from the Cooperative Program for Operational Meteorology, Education and Training (COMET) under a cooperative agreement between the National Oceanic and Atmospheric Administration (NOAA) and the University Corporation for Atmospheric Research (UCAR). The views herein are those of the author, and do not necessarily reflect the views of NOAA, its sub-agencies, or UCAR.

I would like to express my heartfelt thanks to Dr Fuelberg, my major professor, for working with me to complete this research. His efforts, above all others, are responsible for bringing this project to fruition. His guidance, understanding, and most of all patience, are all greatly appreciated. I would also like to thank my other committee members, Dr James O'Brien and Dr Kevin Kloesol. Their insight and guidance were indispensable in writing and presenting this research. I thank you both for the support.

The Air Force Institute of Technology also deserves special recognition. Without them I would never have been able to pursue a Master's degree at Florida State University. I appreciate the trust they had in me to complete this program.

I would also like to thank the forecasters and personnel of the 45 Weather Squadron at Patrick Air Force Base. A few deserve to be singled out for special mention. Top on that list is Mr Bill Roeder. His help in coordinating data requests, setting meeting schedules, and guiding this research is second only to Dr Fuelberg. Also, Mr Clark Pinder and Mr Johnny Weems provided me with operational insights that only years of experience could teach. They have probably forgotten more about Cape Canaveral weather than I will ever know. Lastly, I would like to send a special thanks to Mr Russ Bolton and Mrs Susan

Derussy of Computer Sciences Raytheon. Without there diligent work this project would not have been possible. They went well beyond the call of duty to provide me with the most timely data available. They are a credit to their corporation.

Of course, I cannot forget to thank my lab mates. First, I must thank Anil Rao, my office mate and workout partner, for keeping me focused and healthy. I must thank Scott Longmore for putting up with my endless computer questions and Jeff Cetola for getting me started in this research project. I also thank John Hannan, Rick Lusher, Chris Cantrell, and Jeff Cupo for just being good friends. Your help and encouragement kept me from pulling out what little hair I have left.

Lastly, I must thank my wife, Darci. I simply could not have done this without her.

TABLE OF CONTENTS

LIST OF TABLES

LIST OF FIGURES

ABSTRACT

Warm season thunderstorms represent a significant threat to daily operations at the United States Air Force's (USAF) Cape Canaveral Air Station (CCAS) and the National Aeronautics and Space Administration's (NASA) Kennedy Space Center (KSC) at Cape Canaveral, Florida. Many of these storms are initiated by the East Coast Sea Breeze (ECSB) which forms over the complex land/sea interface around the Cape.

Using data from the 1996-97 warm seasons, 184 sea breeze days were found in the Cape area. To isolate ECSB initiated convection, days were eliminated when outside forcing mechanisms other than the ECSB were indicated. This left 120 days on which only the ECSB affected the area. These days were categorized according to convective activity using NEXRAD reflectivity data and lightning data. The categories were: days when no cells formed along the sea breeze front (NCD), days when cells formed but no cloud-to-ground lightning (CGL) occurred (CD), and days when cells formed and developed into thunderstorms with CGL (LD). Our primary goal was to determine whether one could discriminate between a LD and a CD using 1000 and 1500 UTC radiosonde sounding parameters and surface area-averaged horizontal divergence. Each parameter's ability to forecast a LD versus other days then was assessed. We also documented characteristics of undisturbed ECSB days.

Seven stability parameters from the 1000 and 1500 UTC radiosonde soundings were calculated. Results showed that only the K Index at 1000 UTC statistically discriminated a LD from a CD. Relative Humidity (RH) and u and v wind components from 1000 to 400 mb also were calculated for both sounding times. There were no statistically significant differences in RH between LD and CD at any pressure level for either sounding time. Likewise, the u wind component produced no statistically significant discrimination between the LD and CD categories. However, there were significant differences in the v

component at almost all levels and at both sounding times. The *v* wind component at 700 mb produced the best statistical separation of all parameters studied. There were no statistically significant differences between the temperature profiles of LD and CD for either sounding time.

The forecasting skill of parameters was measured using the True Skill Statistic (TSS). Forecasting skill was based on a forecast of a LD versus a non- LD, i.e., a CD or a NCD. The K index showed the most forecasting skill, followed by the *v* component of the 850 mb wind. Surface area-averaged horizontal divergence (AAD) was found to be of little use as a forecasting tool for undisturbed ECSB initiated convection, both in the nowcasting (0-3 h) or longer term (3-12 h) ranges.

1. INTRODUCTION

Since much of the world's population lives near major bodies of water, it is not surprising that sea breeze research has a long and varied past. References to sea breeze studies can be found as far back as the middle 1600s (Jehn 1973), and the modern scientific literature contains a plethora of model and observational studies. Based on this extensive research, basic characteristics of the sea breeze are well understood (e.g., Pielke 1984; Simpson 1987; Atkins et al. 1995). Fundamentally, the sea breeze is a diurnally occurring, thermally direct, mesoscale circulation caused by differential heating of land and water. The sun typically heats land much faster than water during the morning hours, causing the air just above the land's surface to become warmer and less dense than the air over water. The warmer air tends to rise as the cooler marine air flows inland as a density current. The boundary between the warm, relatively dry air and the cooler, moister marine air is called the sea breeze front (e.g., Simpson 1987). This front is an area of enhanced low-level convergence and upward vertical motion, and it is a preferred location for convection (e.g., Gentry and Moore 1954; Nicholls et al. 1991). In fact, sea breezes and their associated surface convergence are thought to be the dominant mechanism leading to almost daily thunderstorms and precipitation in southern and central Florida from May through October (e.g., Pielke 1974; Byers and Rodebush 1948).

Sea breezes typically form along both the east and west coasts of the Florida peninsula. Inland penetration of the sea breeze is influenced by the low-level synoptic wind flow. Westerly flow pushes the West Coast Sea Breeze (WCSB) inland while keeping the East Coast Sea Breeze (ECSB) close to the eastern shoreline. An easterly flow produces the opposite result. Near calm winds allow both sea breezes to move inland, often meeting near the center of the peninsula (e.g., Byers and Rodebush 1948, Wilson and Megenhardt 1997).

Numerical studies of the sea breeze began in the early 1960s with two-dimensional model simulations (Estoque 1962). This two-dimensional modeling has continued through the present (e.g., Walsh 1974; Bechtold et al. 1991; Nicholls et al. 1991; Xian and Pielke 1991; Arritt 1993). However, the need to simulate complex coastlines and varying synoptic conditions has led to the use of larger, complex three-dimensional models (e.g., McPherson 1970; Pielke 1974; Zhong et al. 1991; Zhong and Takle 1993; Lyons et al. 1995).

While modelers were simulating sea breezes, others were publishing observational and climatological works. Although some lake breezes (e.g., Lyons 1972) are included in these studies, most concentrate on true sea breezes (e.g., Laird et al. 1994; Zhong and Takle 1992; Kingsmill 1995; Laird et al. 1995; Guillory and Jedlovec 1994; Wakimoto and Atkins 1994; Gentry and Moore 1954; Intrieri et al. 1990; Simpson et al. 1977; Blanchard and Lopez 1985). The Florida sea breeze has received major emphasis in the literature. There are three reasons for this emphasis: its almost daily occurrence over the peninsula during the warm months (e.g., Blanchard and Lopez 1985), its link to thunderstorm activity (e.g., Byers and Robenbush 1948; Gentry and Moore 1954; Pielke 1974; Watson et al. 1991), and its impact on operations at the Kennedy Space Center (KSC) and Cape Canaveral Air Station (CCAS) (e.g., Baumann 1995).

Many researchers (e.g., Burpee 1979; Cooper et al. 1982; Ulanski and Garstang 1978) have taken advantage of excellent mesonetwork coverage over parts of southern Florida and large data collecting projects like the Florida Area Cumulus Experiment (FACE) (Woodley and Sax, 1976) to study sea breeze/thunderstorm interactions in the region. Over South Florida, mid-level moisture, low-level wind and stability, and surface convergence have been shown to be the most useful predictors of thunderstorm activity associated with the sea breeze.

The National Aeronautics and Space Administration (NASA) and the United States Air Force (USAF) began space launch operations at Cape Canaveral in the early 1960s (e.g., Manobianco et al. 1996). These operations are extremely sensitive to weather, and thunderstorms in particular pose a serious threat to life and property. There have been numerous studies of thunderstorms and sea breezes for the area. Neumann (1970, 1971a,b) did extensive early work on forecasting thunderstorms at CCAS/KSC. Field

projects like the Convection and Precipitation/Electrification Experiment (CaPE) (Gray 1991) have generated abundant research about thunderstorm activity, and sea breezes in the Cape region (e.g., Wakimoto and Atkins 1994; Atkins and Wakimoto 1994; Laird et al. 1995). Again, mid-level moisture, low to mid-level winds and low-level stability proved to be key ingredients for convection in the Cape Canaveral area.

Other predictors for sea breeze initiated thunderstorms have been found for the Cape area. Wilson and Megenhardt (1997) proposed using across-boundary winds to forecast the degree and location of convective initiation across sea breezes and gust fronts. Furthermore, Watson et al. (1991) used surface divergence signatures to predict the probability and location of lightning strikes. However, Watson et al. (1991) made no distinction as to the cause of the convection that produced the lightning.

To the author's knowledge no study has attempted to quantify the conditions that are most favorable for convective development along the ECSB near Cape Canaveral, or to document what parameters work best to forecast ECSB initiated convection. This paper focuses on the Cape Canaveral ECSB circulation and related convection. Sea breeze days are categorized based on the convection associated with the sea breeze front. These categories are related statistically to stability parameters, winds, relative humidity and surface divergence. The goals are to document the characteristics of the Cape Canaveral sea breeze and to examine ways to improve forecasting convection initiated solely by the ECSB.

2. DATA AND METHODOLOGY

This research focuses on the ECSB circulation and resulting convection that form near Cape Canaveral, Florida. The area of study lies within a 40 km circle centered just southwest of the NASA Shuttle Landing Facility (SLF) (Fig. 1) and covering all of Cape Canaveral, Merritt Island, and parts of mainland Florida. The CCAS and KSC are located on Cape Canaveral and Merritt Island. The USAF 45th Weather Squadron (45WS) is responsible for providing lightning warnings and forecasts for these areas. The 40 km circle in Fig. 1 is positioned to encompasses all of the 45WS lightning warning areas (Pinder 1997, personal communication). The period of study was May through October of 1996 and 1997. The Florida sea breeze is most active during these warm season months (e.g., Nuemann 1971a; Burpee and Lahiff 1984; Cetola 1997).

Forecasting sea breezes and thunderstorms near Cape Canaveral is greatly complicated by the areas physiography, consisting of a complex coastline and extensive inland water bodies (Fig. 1). The Cape itself is a convex landmass that protrudes into the Atlantic Ocean. Separating the Cape from Merritt Island is the Banana River to the southwest and the Mosquito Lagoon to the northwest. The Indian River separates mainland Florida from Merritt Island.

The USAF and NASA have developed an impressive array of sensors to gather mesoscale meteorological data over the area (Fig. 1). Of importance to this study is the mesoscale tower network, the local lightning detection system, Doppler radar coverage from the Melbourne National Weather Service (NWS) WSR-88D (Weather Surveillance Radar-88 Doppler), radiosondes launched from the Cape at 1000 and 1500 UTC daily, and 1 km Geostationary Operational Environmental Satellite (GOES) imagery. A data set of sea breeze days was established using information from these sources. The days then were

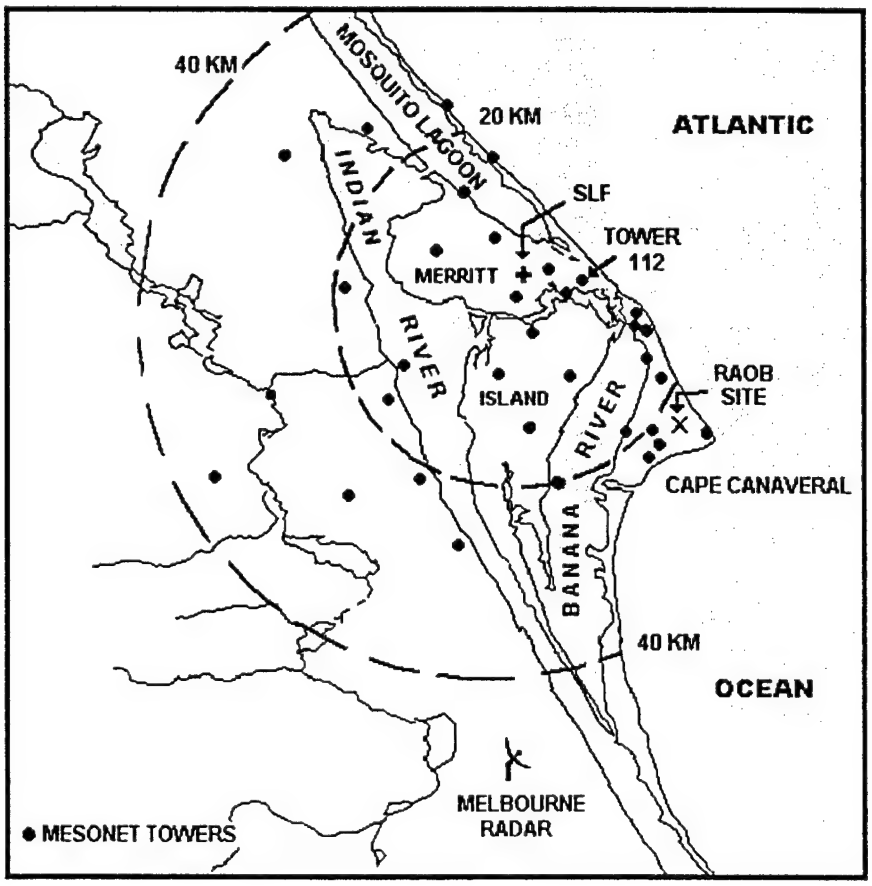

Fig. 1. Map of the Cape Canaveral area. Study area lies within the 40 km radius centered near the SLF. Solid circles indicate locations of mesonet towers used in this study.

screened to remove those on which low-level forcing, other than the ECSB, was indicated. Finally, the data were analyzed for useful forecasting signatures.

a. Data Set

The first step was to identify days with a sea breeze or other boundaries within the study area. Wind measurements from the CCAS/KSC tower mesonetwork were the primary diagnostic tool for this purpose. This network consists of forty-four meteorological towers covering 1600 km^2. The towers report data at heights from 6 to 492 ft; however, each tower is instrumented differently. We used the 54 ft wind reports from the thirty-four towers shown in Fig. 1. This level offered the greatest aerial coverage and is high enough to eliminate surface effects (Watson et al. 1991). The sensors report a 5 min average wind, a 10 min peak wind, and a temperature at 5 min intervals. Similar wind data have been used to identify Cape Canaveral area sea breezes in many previous studies (e.g., Taylor et al. 1990; Zhong and Takle 1993; Laird et al. 1994; Laird et al. 1995; Reed 1979; Zhong et al. 1991; Cetola 1997).

The Spaceflight Meteorology Group (SMG) at NASA's Johnson Space Center, Houston, provided two McIDAS based software packages, XPLOT and TWRJ, to analyze the mesonetwork data. When used together, these tools provide a convenient way to track the development and movement of sea breezes and other boundaries in the study area.

XPLOT displays a time series (meteogram) of wind data at an individual tower. This is useful in determining sea breeze passage because when the sea breeze front passes a tower, there usually is a shift in wind direction to produce a greater on shore component, an increase in wind speed, and a decrease in the variability of wind direction and speed. There often is a slight decrease in temperature and an increase in dewpoint as well. However, all of these characteristics need not, and are not always present with a specific passage. For this research, sea breeze passage time was the time of wind shift when accompanied by sufficient other parameter changes to positively identify the shift as sea breeze related. At times, particularly when synoptic winds were oriented on shore, definite identification of sea breeze formation and passage was impossible. That is, with winds already on shore, sea breeze signatures were sometimes

so weak that it was not possible to determine if, or when, a sea breeze passage had occurred. Such days were not included in our data set. The effects and numbers of these days are discussed later in this section.

In Fig. 2, sea breeze passage at tower 112 (see Fig. 1 for tower location) on 31 July 1997 is clearly indicated by the wind shift at 1610 UTC. The corresponding increase in wind speed and subsequent decrease in temperature verify the sea breeze passage. Following Cetola (1997), we used tower 112 as the reference point for determining sea breeze passage time. Tower 112, located approximately 2 km inland and near the Shuttle Landing Facility (SLF) had the best data availability and is located far enough from inland water bodies to avoid significant influences from river breezes.

While XPLOT was used to examine data at an individual tower, TWRJ provided a spatial view of the entire mesonetwork at a selected time (Fig. 3). This was useful in tracking sea breeze movement, but more importantly, TWRJ plots were used to document secondary convergence zones that developed and affected the sea breeze. These include river breezes, trailing convergence lines, and outflow boundaries.

Under favorable conditions river breezes can form on both the Banana and Indian Rivers (e.g., Laird et al. 1995). River breezes are produced by the same physical processes as the sea breeze, i.e., differential heating of land and water (e.g., Simpson 1994). Numerical simulations have shown that vertical motions associated with the Indian River Breeze (IRB) can be as strong as that of the sea breeze (Zhong et al. 1991). The Banana River Breeze (BRB) has much weaker vertical motions, and no vertical motion has been documented with the Mosquito Lagoon. However, all of these bodies of water can affect the formation and location of convection on and near the ECSB.

An area of enhanced convergence sometimes forms behind the sea breeze front as one section of the sea breeze moves southwest from the northeast coast and meets the section of the sea breeze moving northwest from the southeast coast. Laird et al. (1995) and Cetola (1997) give a complete discussion of this phenomenon. The resulting line of convergence, called a Trailing Convergence Line (TCL) can be a focus of low-level convergence and enhanced convection (Laird et al. 1995). The formation of river breezes and TCLs were tracked in this study. The role of outflow boundaries will be discussed shortly.

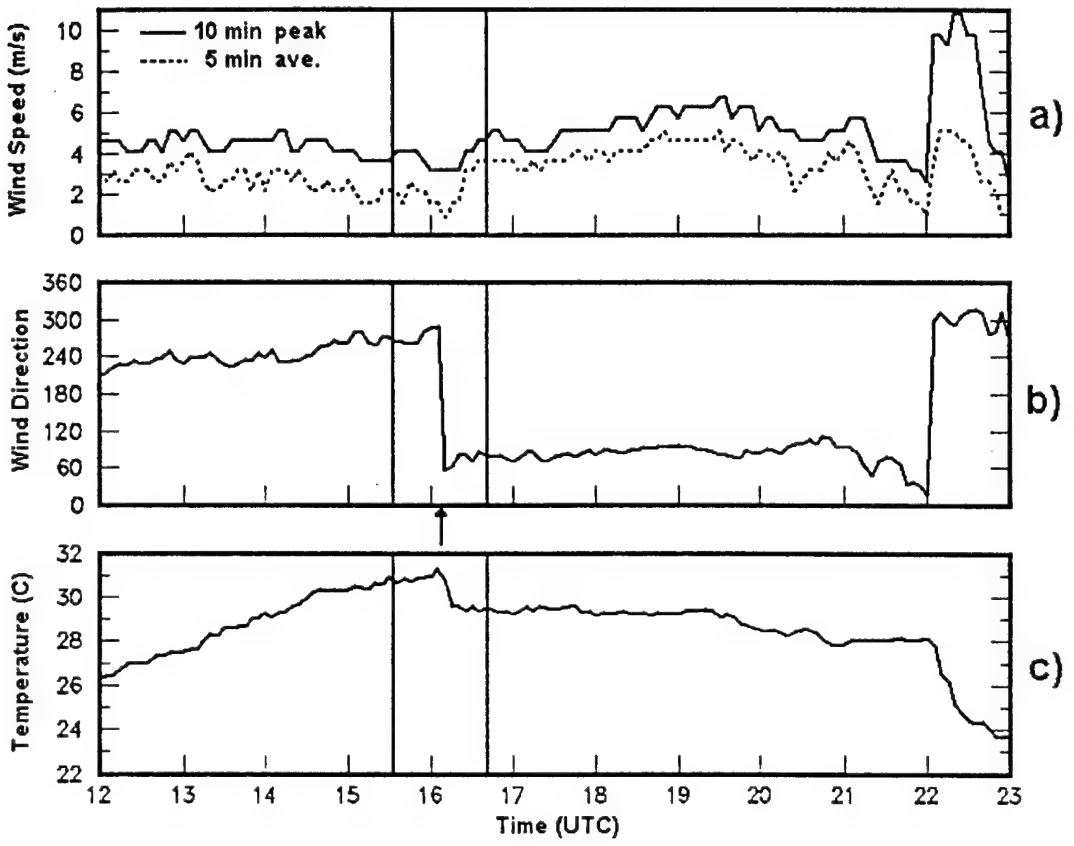

Fig. 2. Meteograms of 54 ft data for tower 112 on 31 July 1997: a) wind speed, b) wind direction, and c) temperature. Bracketed period includes sea breeze passage signatures. Arrow marks time of recorded sea breeze passage. Note the increase in wind speed, wind shift, and drop in temperature.

The day 24 June 1997 is an example of the above mentioned phenomena. On that day, a sea breeze, two river breezes, a TCL, and an outflow boundary all developed within or moved through the study area. Four TWRJ plots from 24 June are shown in Fig. 3. In the morning (1200 UTC) all winds are light and offshore. By 1730 UTC, the sea breeze has formed and moved approximately 10 km inland. Also at this time, river breezes have formed over the Indian and Banana rivers as indicated by the divergent flow off the water. This is verified in satellite images as clear zones over both rivers (not shown). By 1900 UTC, the sea breeze is almost to the Indian River. The BRB has been swept away by the passage of the sea breeze, and a weak TCL has formed behind the sea breeze front as indicated by the convergent wind flow over the Cape and part of Merritt Island. By 2150 UTC the sea breeze is west of the study area, and an outflow boundary from the northwest has moved through the northern half of the CCAS/KSC tower network.

Of the 368 days comprising the 1996-97 warm seasons, 340 days could be analyzed using the above techniques for sea breeze formation. The remaining 28 days were unusable due to data loss (16 days) or the inability to accurately determine if a sea breeze developed during cases of onshore flow (12 days). Sea breezes were found on 54 percent (184) of the 340 days. This is only slightly less than the 60 percent found by Cetola (1997) durning the 1995 warm season. Based on this result and the similarity of our large-scale flow (refer to chapter 3 part b) to those of Neumann's (1970) 13 year study, it appears that 1996 and 1997 were representative years for the area.

Starting the study period on 1 May and ending on 31 October allowed us to compare 1996 and 1997 with previous years. However, this period was not optimal for the remainder of the research because the first weeks of May and all of October have relatively few sea breeze days and their wind, temperature, and humidity profiles often do not resemble summertime conditions. Since our objective was to examine true warm season situations, the study period was shortened to start with the first day that lightning occurred with sea breeze related convection in May and end with the last day lightning occurred with a sea breeze before 31 October. For 1996 these dates were 26 May to 30 September and for 1997 they were 19 May to 2 October. This left 237 usable days. Sea breezes were found on 70 percent (165) of these days.

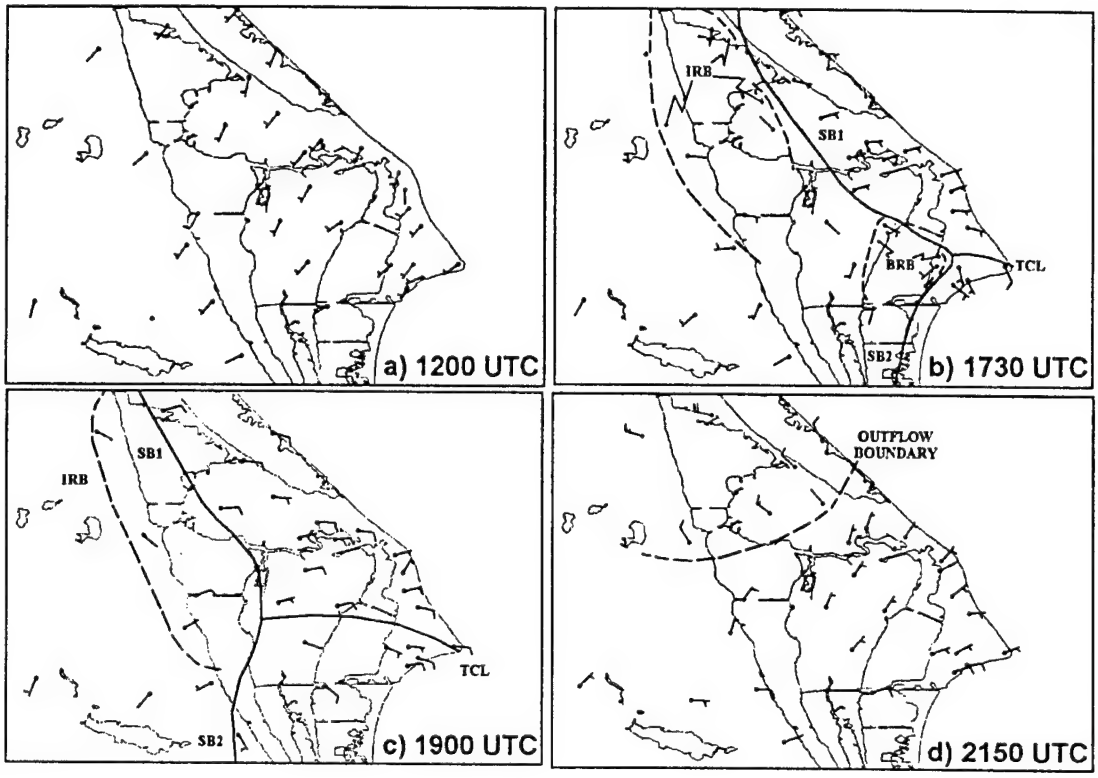

Fig. 3. TWRJ plots for 24 June 1997. Short (long) wind barbs denote speeds of 2.5 (5.0) m s^{-1}.

Each of the 165 sea breeze days was categorized as either a no cell day (NCD), cell day (CD), or lighting day (LD) based on WSR-88D base reflectivity imagery and lightning data. If the sea breeze did not cause convective cells to form within the study area, the day was categorized as a NCD. If convective cells developed along the sea breeze as it moved through the area, but no cloud-to-ground lightning (CGL) occurred, the day was categorized as a CD. If convective cells formed and matured into thunderstorms producing CGL, the day was categorized as a LD.

Lightning data were from a local lightning detection system used by the 45WS, i.e., the Cloud-to-Ground Lightning Surveillance System (CGLSS) (Harms et al. 1997). CGLSS has an effective range of 100 km, a strike detection accuracy of 92 percent and a location accuracy of 0.5 km. The system reports time of strike, its location, and polarity.

Radar imagery from the Melbourne NWS WSR-88D, located south of the Cape (Fig. 1), was used to identify cell formation. A cell was defined as a localized area of at least 24 dBZ returned power that reached the fourth scan level (3.3° elevation) and lasted at least 15 consecutive minutes above the second scan level (1.4° elevation). The cell was required to develop within 5 km of the sea breeze signature, the line of weak echoes in the first scan level (0.4° elevation). Otherwise that day was considered disturbed, i.e., some mechanism other than the ECSB was causing the convection. Since our objective was to study days on which the first convection was caused by the ECSB, such disturbed days were not used.

Days also were eliminated if outside, low-level forcing mechanisms such as outflow boundaries entered the mesonetwork. (River breezes and TCLs that developed within the network were considered part of the local sea breeze mechanism, as were outflows produced by sea breeze initiated cells.) This screening was done using 1 km GOES visible satellite imagery, WSR-88D imagery, and TWRJ wind plots. The satellite imagery provided a large area view to detect thunderstorms producing outflows that moved into or near the study area. The radar products revealed outflows that did not produce visible cloud features. TWRJ provided ground truth to the above methods. After these final screening processes, 120 usable sea breeze days remained for the two warm seasons. These days constitute the final data set of the study.

b. Analysis

Since the large scale, low-level wind flow has been shown to have a significant impact on the sea breeze and convection in Florida (e.g., Zhong and Takle 1993; Estoque 1962; Bechtold et al. 1991; Xian and Pielke 1991; Neumann 1977; Blanchard and Lopez 1985; Lopez and Holle 1987a; Zhong et al. 1991; Wakimoto and Atkins 1994; Atkins et al. 1995), sea breeze days were classified based on the mean vector wind in the 300-900 m layer from the 1000 UTC KSC sounding. This level was chosen because it encompasses the majority of the sea breeze circulation and is used by 45 WS forecasters to determine the large-scale flow (Roeder 1997, personal communication).

Following the classification scheme of Lopez and Holle (1987b) and Watson et al. (1991), mean wind categories were based on the coastal geography of the Cape. Specifically, the categories utilized 90° sectors centered on directions perpendicular to (68° and 248°) and parallel to (158° and 338°) the average coastline near Cape Canaveral (Fig. 4). Thus, winds from 294° - 023° were classified as northwest (NW), winds from 024° - 113° as northeast (NE), winds from 114° to 203° as southeast (SE), and winds from 204° to 293° as southwest (SW). Days with speeds less that 2 m s^{-1} were classified as calm.

We also examined the type of sea breeze that formed each day. Three distinct types of sea breezes develop near the Cape, based on the way the sea breeze advances inland. If the sea breeze propagates primarily from the northeast, it is designated NE-type. Conversely, if it propagates primarily from the southeast, it is SE-type. A third type occurs when a sea breeze moves in from the northeast and southeast at the same time; it is called the SB1/SB2-type (Laird et al. 1994). SB1/SB2 days often lead to TCL formation as discussed above.

We examined several stability parameters in an attempt to determine those that best discriminate between convection categories and to determine those with the best forecasting skill. The 45WS forecasters routinely use the K-Index, Lifted Index and Total Totals (Pinder 1997, personal communication) as predictors of general convection. NWS forecasters at Melbourne recently have been testing Convective Available Potential Energy (CAPE) as a predictor (Sharp 1997, personal communication). Bauman (1995) suggested that Convective Inhibition (CIN) might be a useful

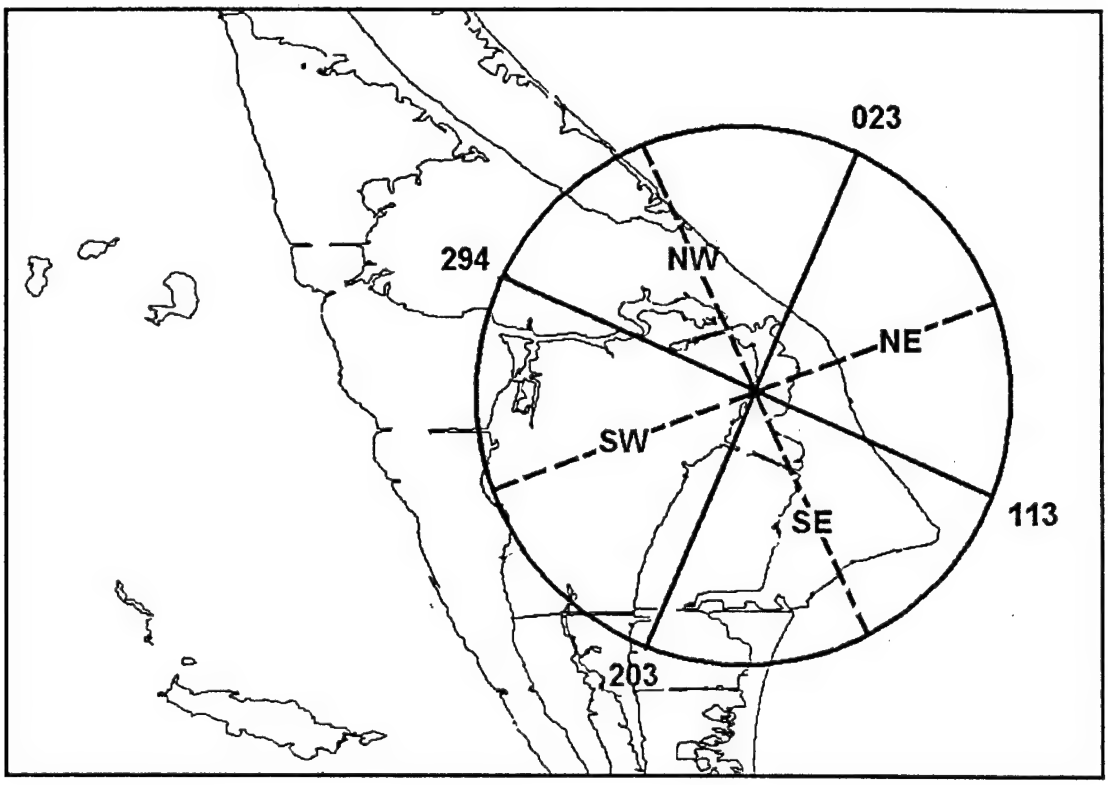

Fig. 4. Quadrants for typing the large-scale wind direction near Cape Canaveral, Florida. For example, the northwest (NW) quadrant ranges from 294° to 023°.

predictor in easterly flow regimes. Neumann (1971a) used the Showalter Index to develop a local stability index for the Cape area. Fuelberg and Biggar (1996) also studied the Showalter Index as a predictor of convection in the Florida Panhandle. Lastly, the Level of Free Convection (LFC) also was examined. All stability parameters were calculated using GEneral Meteorological PAcaKage (GEMPAK) routines from the National Centers Advanced Weather Interactive Processing System (N-AWIPS). For the Lifted Index, the parcel being lifted was the layer 100 m above the surface. For CAPE and CIN the lifted parcel was the lowest 500 m of the atmosphere.

The 54 ft winds from the CCAS/KSC mesonetwork (Fig. 1) were used to calculate Area-Averaged horizontal Divergence (AAD) following the technique of Watson et al. (1991). Watson et al. (1991) found that a sharp, semi-continuos drop in AAD often preceded lightning strikes. Two such events on 25 June 1996 are shown in Fig. 5. Each sharp drop indicated in the figure was followed by lightning strikes in the study area. Watson et al. (1991) proposed that area-averaged divergence be used as a nowcasting (0-3 h) tool for lightning at the Cape. Forecasters at the 45WS currently look for such a trend to issue lightning warnings (Pinder and Roeder 1997, personal communication). The current study examines the feasibility of using area-averaged divergence data as both a short-term forecasting (6-12h) and nowcasting (0-3h) tool for ECSB convection.

It was important to determine statistically which parameters best distinguished between the three categories of convection. The usual procedure is to test for differences in the means of the categories. The standard test to determine statistical significance between means is the t-test. However, this test assumes that the data follow a normal distribution, and with a small data set, assumes equal standard deviations. Since our data did not always satisfy these assumptions, the t-test was not appropriate. Instead, we used a non-parametric test called Multi-Response Permutations Procedures (MRPP) (Mielke et al. 1976, 1981) that makes none of the above assumptions about data distribution. Mielke et al. (1981) describe the technique and its application to a meteorological problem. Blanchard and Lopez (1985) successfully used MRPP with data similar to ours. MRPP compares data groups to determine if they are from separate

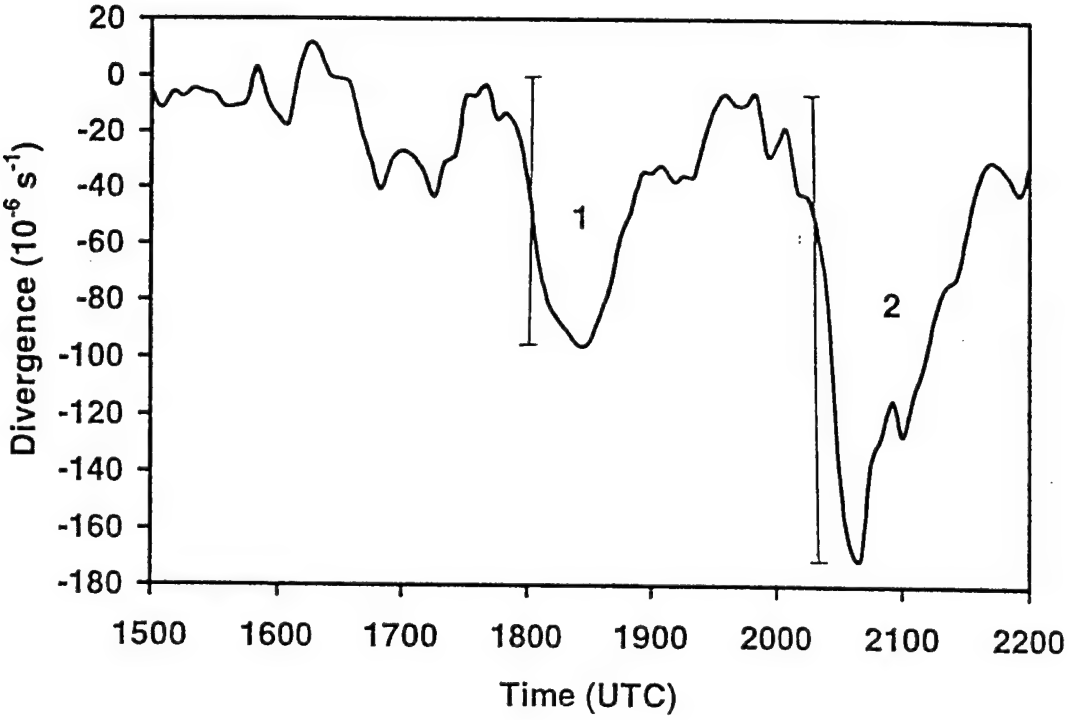

Fig. 5. Two examples of convergence events that lead to lightning strikes on 25 June 1996. These are typical patterns as discussed by Watson et al. 1991. The vertical lines indicate the overall change in the divergence for each event.

populations and gives a p-value result of statistical significance. Typically, a p-value ≤ 0.05 allows one to reject the hypothesis that the data are from the same population. Stated another way, a p-value ≤ 0.05 allows one to say that the data came from different populations at the 95 percent or higher confidence level. The MRPP was applied to the stability parameters, RH, and u and v wind components from the 1000 and 1500 UTC soundings. (The u and v wind components were used to avoid problems with direction based on the 360° compass.)

The occurrence of serial correlation was addressed before statistical significance was assessed. Serial correlation often is a problem with daily meteorological data. As an example, Burpee and Lahiff (1984) found mean rainfall values in South Florida to be highly correlated with rainfall on the previous day. Such a relationship suggests high serial correlation in the data. In other words, one cannot assume that day-to-day data are independent. To minimize this problem, a subset of the original data was used. Days were chosen such that a minimum of a 6-day gap existed between successive entries in any category. Other days were deleted from the data set. This procedure was not utilized in calculations that did not involve statistical significance.

The MRPP does not quantify the accuracy of a forecast based on the various parameters. A different statistical procedure is required for this purpose. We evaluated the ability of parameters to successfully forecast a LD versus CD or NCD using the True Skill Statistic (TSS) described by Watson et al. (1991) and Doswell and Flueck (1989), and used by Fuelberg and Biggar (1994). Since the TSS requires only two possible outcomes (i.e., lightning either did or did not occur) we combined the CD and NCD groups. In this application the TSS is defined as

$$TSS = POD - POFD,$$

where POD, the Probability Of Detection, and POFD, the Probability Of False Detection, are defined as

$$POD = FLDO / TLDO,$$

and

$$POFD = FLDNO / TNLDO,$$

where FLDO represents Forecast LD -- Observed (i.e., correct LD forecasts), TLDO represents the Total of LD -- Observed (i.e., total days in LD category), FLDNO represents Forecast LD -- Not Observed (i.e., incorrect LD forecasts), and TNLDO denotes the Total of Non-Lightning Days -- Observed (i.e., all days in the combined CD and NCD categories). The TSS offers several desirable characteristics. It considers all aspects of 2 X 2 contingency tables and compares actual forecast performance to perfect performance, with a fixed range between –1 and +1, where +1 indicates a perfect forecast.

3. RESULTS

The final set of 120 undisturbed ECSB days from the 1996–97 warm seasons consists of 49 percent LD (59 days), 24 percent CD (29 days), and 27 percent NCD (32 days). One should note that nearly half of the days produce a lightning strike within 40 km of the SLF. Unlike storms that form inland and move eastward toward the Cape, these strikes are from storms that develop in the area. Thus, there usually is little opportunity to "see it coming". This illustrates the importance of developing better techniques to forecast the formation of convection on the ECSB.

Statistical comparisons are presented in this chapter. As stated earlier, a subset of the data was used to minimize serial correlation. For MRPP comparisons the sample sizes are 24 LD, 15 CD, and 17 NCD. All other results use the full data set.

a. Sea Breeze Characteristics

There is little differentiation in event timing between convection categories (Table 1). For example, the mean time of sea breeze passage at tower 112 is near 1530 UTC for each category. The earliest passages also are similar, about 1245 UTC in all three cases, while the latest passage ranges from 1810 UTC for CD to 2110 UTC for NCD. Mean times of cell formation for LD and CD are the same, 1629 UTC. These timing characteristics are similar to climatological values for all ECSB days, disturbed or otherwise. Cetola (1997) found that the average sea breeze passage time at tower 112 is 1528 UTC, with the earliest (latest) passage time of 1210 UTC (2120 UTC).

When the ECSB days are grouped according to the type of synoptic flow (Fig. 6a), there is better discrimination between convection categories. LD are most common during the SW and SE flow regimes, i.e., 60 percent of days with SW winds are LD, while 54 percent of days with SE winds are LD. This is

Table 1. Statistics on time of ECSB passage at tower 112 and cell development. All times UTC.

		Mean	Latest	Earliest	Standard Deviation
Time of ECSB Passage	LD	1547	1845	1230	1:36
	CD	1502	1810	1245	1:34
	NCD	1527	2110	1250	1:57
Time of First Cell	LD	1629	2105	1320	1:39
	CD	1629	2010	1255	1:56

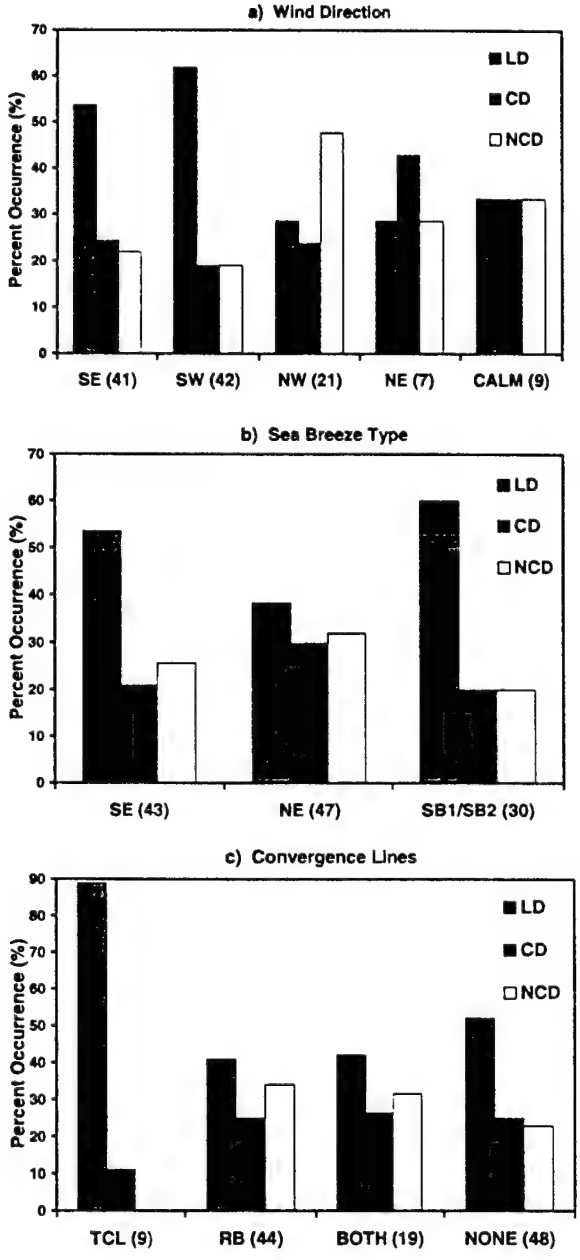

Fig. 6. Distributions by a) wind flow type, b) sea breeze type, and c) occurrence of TCL and river breezes for LD, CD, and NCD. Numbers in parenthesis indicates total days per category.

consistent with previous studies (e.g., Cetola 1997; Neumann 1971b). Lightning is not common during NW flow. In fact, almost half (48 percent) of NW flow days are NCD and only 28 percent are LD. Watson et al. 1991 found a similar lack of lightning events for NW flow days. NW flow normally is post frontal and therefore more stable, resulting in the lack of convection. NE flow is uncommon and is normally characterized by moist surface flow capped by descending motion aloft (Watson et al. 1991).

Sea breeze typing (Fig. 6b) also produces noticeable differentiation between categories. Over half (53 percent) of SE sea breeze days are LD; however, LD, CD, and NCD are more evenly distributed among NE flow days. Also, 60 percent of days with a SB1/SB2 sea breeze are categorized as LD. These findings are consistent with those of Cetola (1997).

If a TCL forms, it is likely that ECSB generated convection will cause a lighting strike within the study area (Fig. 6c). However, since there were so few TCL days (only 9 total), these results may not be representative. Nonetheless, this finding does agree with Cetola (1997) who found that TCL days had an increased likelihood of convection and with Laird et al. (1994 and 1995) who noted that TCLs play an important role in initiating convection. Days having river breezes or both river breezes and TCLs (Fig. 6c) generally show few differences among categories.

b. Sounding Parameters

Our first step in examining the 1000 and 1500 UTC radiosonde soundings was to produce composite vertical profiles of wind, relative humidity, and temperature. (Composite wind direction was calculated from the vector averaged u and v winds. Composite wind speed was averaged from reported speeds.)

1. Wind. Fig. 7a shows composite wind speed profiles from the 1000 UTC soundings. Differences between categories are less than 2 m s^{-1} below 600 mb. The LD profile exhibits the least vertical variability, staying between 4.5 and 6.0 m s^{-1} throughout the sounding. Above 500 mb, the CD and NCD profiles show increasing speeds, while LD speeds decrease slightly. Although the best differentiation

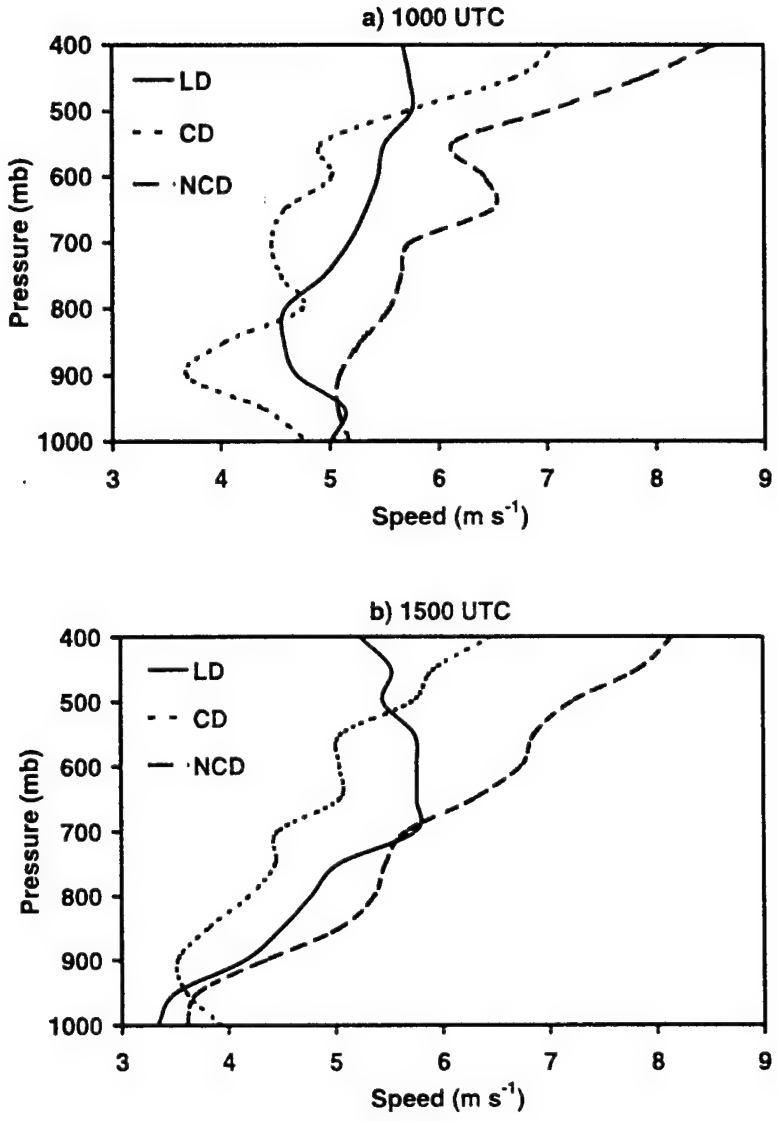

Fig. 7. Composite wind speed profiles at a) 1000 UTC and b) 1500 UTC.

occurs at 400 mb, this difference is only approximately 3 m s^{-1}. Unfortunately, there was insufficient data above 400 mb to continue the profiles.

The 1500 UTC composite wind speed profiles (Fig. 7b) are very similar to those 5 hours earlier (Fig. 7a). There is little differentiation below 600 mb. LD again decrease in speed above 600 mb, while CD and NCD increase. At both 1000 and 1500 UTC, mean NCD wind speeds are strongest throughout most of the sounding. This is likely the effect of climatologically stronger winds in May and September which are the months having the greatest numbers of NCD. Above 500 mb, LD have weaker winds than the other two categories. The difference between LD and NCD is on the order of 3 m s^{-1} in at 400 mb for both times.

Composite wind direction profiles for 1000 UTC are given in Fig. 8a. LD exhibits minimal directional wind shear throughout the sounding, i.e., direction remains between 210° and 260°. However, both CD and NCD have large northerly components between 900 - 750 mb. Our LD profile is similar to the Type 3 profile derived by Blanchard and Lopez (1985) from the 1200 UTC Miami sounding. Their Type 3 days were characterized by early, widespread convection along both Florida coasts, a southwesterly mean wind that keeps the ECSB close to the coast, and a WCSB that moves quickly inland. Our results suggest that the Type 3 regime is favored for undisturbed ECSB convection. This agrees with the wind distribution shown in Fig. 6a where LD have the greatest percentage of occurrence for southwest flow. However, our CD and NCD profiles show no similarities to other Blanchard and Lopez (1985) typing regimes.

The 1500 UTC composite direction profile (Fig 8b) is similar to the 1000 UTC profile. This is not surprising since there is only five hours between sounding times.

Frequency distributions of wind speed are nearly the same for all three convection categories. This is true at both 1000 and 1500 UTC and at all levels. A representative example is the 850 mb speed distribution at 1000 UTC (Fig. 9a). The frequency distribution of wind direction at 850 mb (Fig. 9b) does show good separation between categories. LD are most common in the 200° - 239° range. CD and NCD are more evenly distributed around the compass.

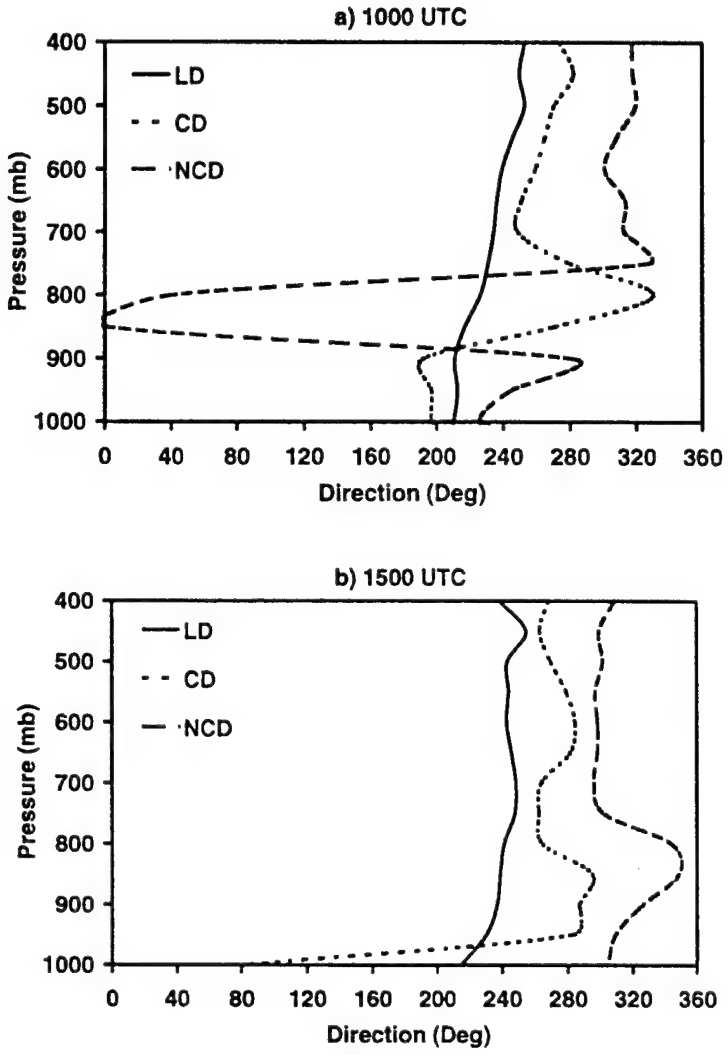

Fig. 8. Composite wind direction profiles at a) 1000 UTC and b) 1500 UTC.

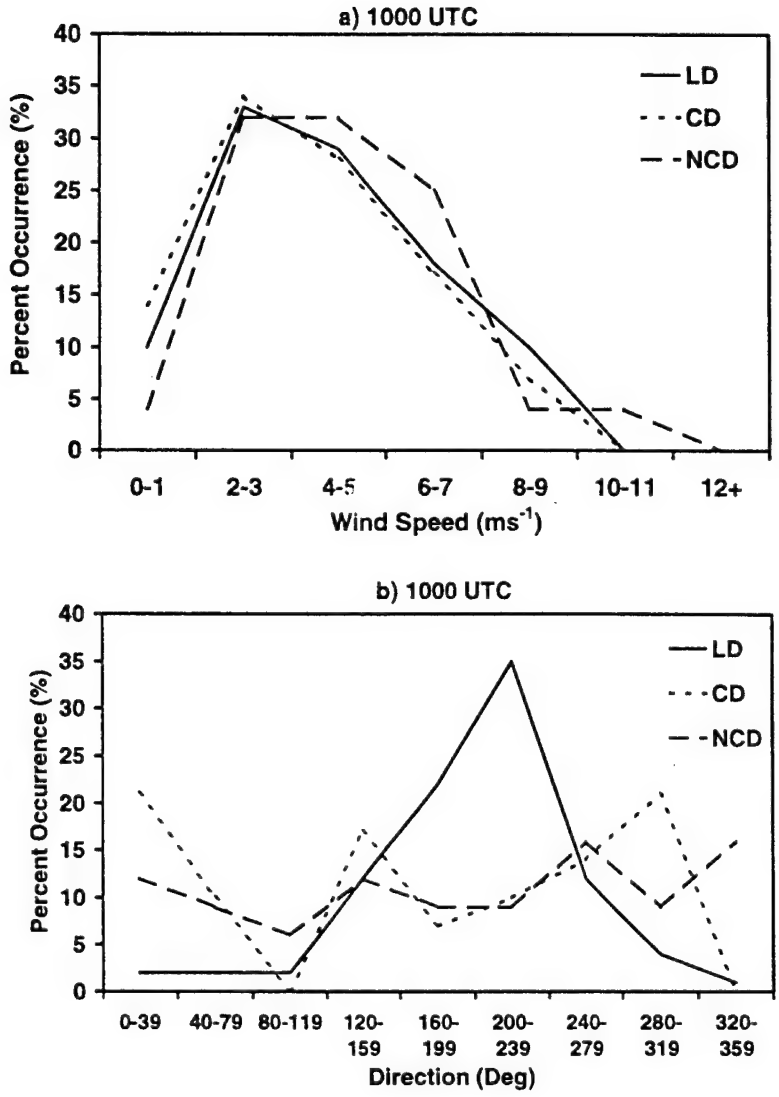

Fig. 9. Frequency distributions for 850 mb a) wind speed and b) wind direction at 1000 UTC.

To determine statistically whether the wind is a good discriminator between convective categories, MRPP was applied to the *u* and *v* wind components. Two comparisons are made: LD versus CD, and LD versus a combined CD and NCD group. The LD versus CD is the more difficult comparison and the one of most interest in this study. That comparison is described in the following sections unless otherwise noted. The LD versus combined CD and NCD comparison is included as a baseline and because forecasting statistics presented later in this chapter require that these groups be combined.

MRPP results for the *v* wind are shown in Table 2. The *v* wind is a good discriminator of LD versus CD at 1000 UTC. Between 900 and 500 mb, *v* winds for the two categories are significantly different (p-values ≤ 0.05.) The best results are at the 700 and 750 mb levels with p-values of 0.001 and 0.003, respectively. At 1500 UTC, the best discrimination occurs at 850 mb (a 0.004 p-value).

MRPP results for the *u* component (not shown) show no statistically significant differences between categories. This might seem surprising at first, but due to the screening process, days with strong *u* winds were deleted from the data set. If the wind has a strong westerly component, then a) the ECSB never forms, or b) the WCSB races across the peninsula and disturbs the ECSB. Conversely, if the wind has a strong easterly component, then a) the ECSB never forms, or b) the sea breeze races quickly inland taking any convection with it. This process effectively deleted extremes in *u* winds from the data set, thus limiting its variability from one category to the next. However, this information still is useful to a forecaster since days with strong absolute values of the *u* wind are not likely to have undisturbed ECSB convection.

The MRPP results (Table 2) indicated that the 700 mb *v* wind component at 1000 UTC is statistically best at discriminating convective development along the ECSB. To quantify the accuracy of forecasts based on that parameter the TSS was calculated. Results are shown in Table 3. TSSs were calculated using an iterative process to determine the threshold value that produced the highest score. For the 700 mb *v* wind component, the threshold of -1.0 m s^{-1} produces a 0.29 TSS. Although the 700 mb *v* component shows the best separation based on MRPP, the 850 mb wind actually produces the best TSS score, 0.43, based on a threshold of 0.5 m s^{-1}. The fact that the 850 mb wind produces a better

Table 2. MRPP results. The p-values ≤ 0.05 are in bold italic type. They indicate statistical significance at the 95 percent level or higher.

	1000 UTC		1500 UTC	
	p-value (LD vs CD)	p-value (LD vs CD + NCD)	p-value (LD vs CD)	p-value (LD vs CD + NCD)
v Wind Component				
500 mb	***0.0500***	***0.0030***	0.1800	0.0800
550 mb	***0.0500***	***0.0100***	***0.0400***	***0.0100***
600 mb	***0.0300***	***0.0090***	0.1000	***0.0070***
650 mb	***0.0090***	***0.0040***	***0.0500***	***0.0030***
700 mb	***0.0010***	***0.0006***	***0.0200***	***0.0020***
750 mb	***0.0030***	***0.0010***	***0.0200***	***0.0009***
800 mb	***0.0100***	***0.0080***	***0.0050***	***0.0002***
850 mb	***0.0300***	***0.0020***	***0.0040***	***0.0003***
900 mb	***0.0100***	***0.0004***	***0.0120***	***0.0005***
950 mb	0.0600	***0.0030***	***0.0060***	***0.0003***
1000 mb	0.2800	***0.0400***	***0.0110***	***0.0005***
Point Value RH				
400 mb	0.9500	0.1200	0.5000	***0.0005***
450 mb	0.6200	0.1900	0.4800	0.5000
500 mb	0.7400	0.5400	0.1800	0.1000
550 mb	0.2500	0.0800	0.2000	***0.0100***
600 mb	0.3600	0.1100	0.1200	***0.0300***
650 mb	0.5400	0.0800	0.2400	***0.0300***
700 mb	0.0700	***0.0400***	0.1800	***0.0070***
750 mb	0.9500	0.6800	0.8000	0.4600
800 mb	0.8800	0.1800	0.8200	0.6700
850 mb	0.1200	***0.0400***	0.1800	***0.0090***
900 mb	0.0900	***0.0400***	0.6000	0.0700
950 mb	0.1900	0.0700	0.5800	0.1900
1000 mb	0.6500	0.2000	0.6100	*0.3000*
Stability				
K Index	***0.0040***	***0.0200***	0.2100	***0.0200***
Lifted Index	0.2000	***0.0040***	0.1400	***0.0006***
Showalter Index	0.4100	0.0600	0.2500	***0.0060***
Total Totals	0.4100	0.1100	0.7900	***0.0400***
CAPE	0.9800	0.1600	0.0900	0.0900
CIN	0.1900	0.1100	0.3200	***0.0300***
LFC	0.7200	0.1000	0.2800	0.1700

Table 3. TSS contingency tables.

	Observed Category		
Predicted Category	**LD**	**CD + NCD**	**Total**
700 mb v wind (1000 UTC)			
LD ($\geq$ -1 m s^{-1})	44	33	77
CD + NCD (< -1 m s^{-1})	8	26	34
Total	52	59	111
	POD = 0.85	**POFD** = 0.56	**TSS** = 0.29
Predicted Category	**LD**	**CD + NCD**	**Total**
850 mb v wind (1000 UTC)	41	21	62
LD ($\geq$ 0.5 m s^{-1})	11	38	49
CD + NCD (< 0.5 m s^{-1})	52	59	111
Total			
	POD = 0.79	**POFD** = 0.36	**TSS** = 0.43
Predicted Category	**LD**	**CD + NCD**	**Total**
700 mb RH (1000 UTC)			
LD ($\geq$ 70%)	43	21	87
CD + NCD (< 70%)	9	38	24
Total	52	59	111
	POD = 0.83	**POFD** = 0.36	**TSS** = 0.47
Predicted Category	**LD**	**CD + NCD**	**Total**
K Index (1000 UTC)			
LD ($\geq$30 °C)	40	11	51
CD + NCD (<30 °C)	12	48	60
Total	52	59	111
	POD = 0.77	**POFD** = 0.19	**TSS** = 0.58
Predicted Category	**LD**	**CD + NCD**	**Total**
Area-Averaged Divergence			
LD ($\geq$ 75 units)	41	38	79
CD + NCD (< 75 units)	12	21	32
Total	53	59	111
	POD = 0.79	**POFD** = 0.64	**TSS** = 0.15

forecast agrees with the wind directions profile (Fig. 8a) where the greatest difference between categories is indicated near to 850 mb. It is not surprising that the threshold value is near 0.0 m s^{-1}. The wind speed distribution (Fig. 9a) shows little difference in wind speeds between convective categories, and the composite direction profiles (Fig. 8a) show that the LD category has a southerly (i.e., negative v) wind component while both non-LD categories have a northerly (i.e., positive v) component.

2. Relative Humidity. Composite relative humidity profiles for 1000 UTC (Fig. 10a) are similar below 900 mb. This is due to the continuously high humidity in the lower troposphere throughout the warm months. However, from 900 to 400 mb there is good separation, with LD more humid than CD and NCD. For example, at 700 mb the LD average RH is 63 percent, the CD average is 47 percent, and NCD average is 40 percent. This contrast is consistent with the findings of Frank and Smith (1968), Burpee (1979), Lopez et al. (1984). That is, mid-tropospheric moisture is one of the best predictors of summertime precipitation in Florida. At 1500 UTC (Fig. 10b), the separation still is good above 750 mb. At 700 mb, LD RH is 65 percent, CD is at 55 percent, while NCD is still at 40 percent. Of the two sounding times, the 1000 UTC RH frequency distribution for 700 mb (Fig. 11) shows the best separation between categories. The greatest occurrence of LD is associated with RH between 60-69 percent.

RH does not exhibit statistically significant discrimination between LD and CD at any height or either sounding time (Table 2). The 700 mb RH at 1000 UTC performs best with a 0.07 p-value. For the LD versus CD + NCD comparison at 1000 UTC, RH shows better differentiation, particularly near 850 and 700 mb. There is even better discrimination at 1500 UTC, with a 0.007 p-value at 700 mb. These results are consistent with the works mentioned earlier (Frank and Smith 1968, Burpee 1979, and Lopez et al 1984b) that found mid-level moisture to be a good predictor of precipitation in Florida. In terms of forecast skill for LD versus CD, 700 mb RH at 1000 UTC produces the best TSS: 0.47 based on a threshold value of 70 percent (Table 3). This is slightly larger than the TSS of the v wind component at 850 mb (0.43).

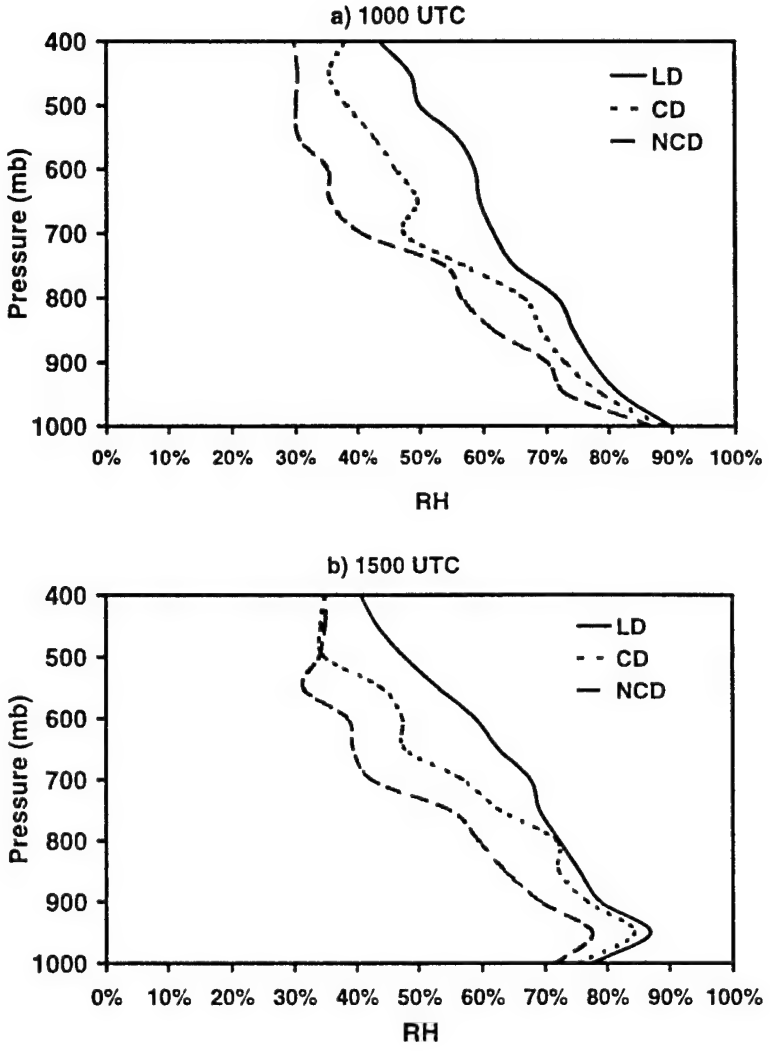

Fig. 10. Composite RH profiles at a) 1000 UTC and b) 1500 UTC.

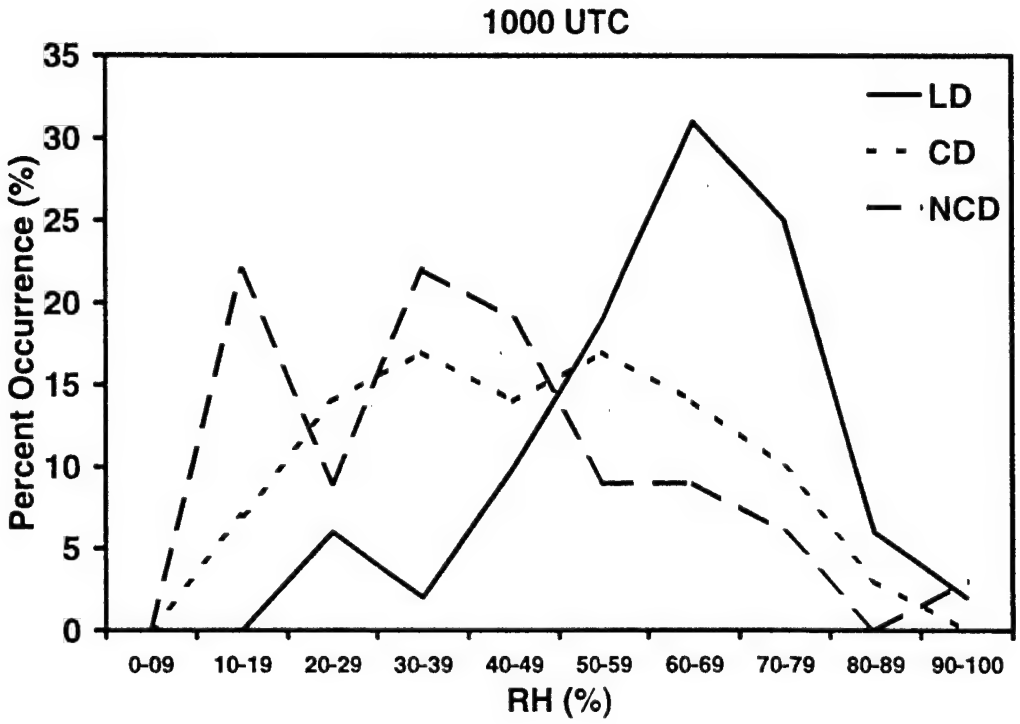

Fig. 11. Frequency distributions for 700 mb RH at 1000 UTC.

3. Temperature. Composite vertical temperature profiles for the convection categories are almost identical (not shown). To better reveal any possible differences, we subtracted the mean temperature profile for each category from the mean profile of the entire data set. Results illustrate the small variations (Fig. 12a, b). At 1000 UTC, the maximum separation between categories, ≈ 0.7°C, is between LD and CD at 950 mb. LD are cooler than the overall mean below 700 mb, while CD are warmer below 500 mb; however, the differences are less than 0.5°C in both cases. Such small contrasts are essentially useless as a distinguishing characteristic for the operational forecaster. Burpee (1979) found that temperatures between 850 and 450 mb over South Florida were consistently cooler for rainier than average sea breeze days. However, this is not indicated for undisturbed ECSB days near the Cape. Only below 850 mb are CD and NCD consistently warmer than LD. Results at 1500 UTC (Fig. 12b) generally are similar to those at 1000 UTC. The slightly larger difference between LD and CD at 800 mb, is still less than 1°C. These results are consistent with those for the Florida panhandle (Fuelberg and Biggar 1994) which showed a similar lack of distinction in the temperature profiles for strong convective days versus weak convective or non-convective days. MRPP significance tests confirm the lack of temperature distinction between categories (not shown).

4. Stability. Table 4 gives mean, maximum, minimum, and standard deviations for the stability parameters we examined. Mean values of LFC at 1000 UTC show little differentiation between LD, CD, and NCD. Mean LFC values are lowest on CD (879 mb) and highest on NCD (814 mb). Frequency distributions of LFC (Fig. 13a) are similar for the three convective categories. Statistically (Table 2), LFC is one of the worst discriminators of LD versus CD with a 0.72 p-value. While p-values are smaller at 1500 UTC they still do not indicate statistically significant differences.

Mean values of CIN (Table 4) indicate that it may be good at separating NCD from the other categories (-61 for NCD versus –32 for LD and –25 for CD at 1000 UTC). However, CIN offers little hope for differentiating CD from LD. Like LFC, the frequency distributions of CIN (not shown) all are similar and the MRPP p-value at 1000 UTC (0.19) does not indicate a significant difference between categories (Table 2).

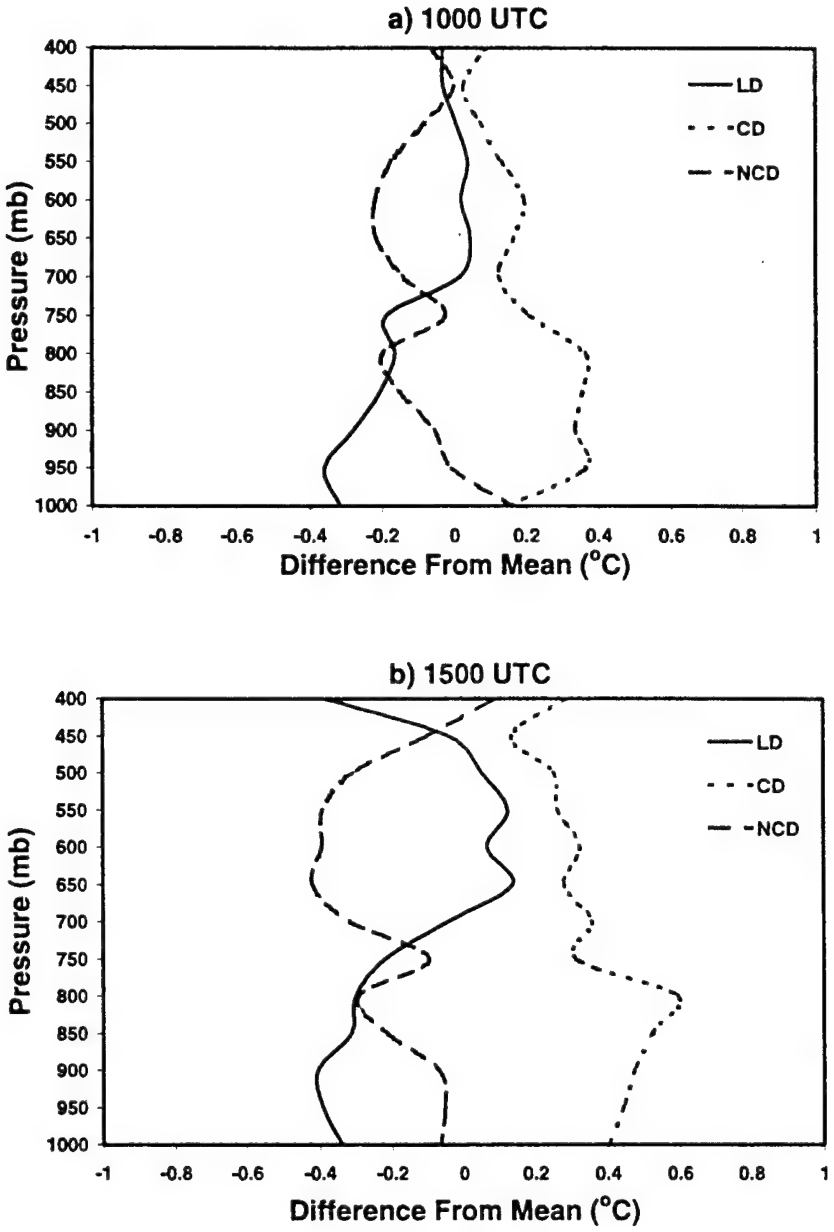

Fig. 12. Vertical profiles of mean temperature differences between each day's a) 1000 UTC and b) 1500 UTC sounding and the average of all undisturbed ECSB days.

Table 4. Statistics on stability parameters.

		1000 UTC				1500 UTC			
		Mean	Maximum	Minimum	Standard Deviation	Mean	Maximum	Minimum	Standard Deviation
	LD	30	38	8	6	31	40	9	6
K Index	CD	24	38	2	9	27	38	1	8
(°C)	NCD	19	33	-7	10	21	33	-6	10
	LD	-4	-1	-8	2	-5	0	-8	1
Lifted Index	CD	-3	2	-7	2	-4	4	-6	2
(°C)	NCD	-2	3	-5	3	-2	5	-5	2
	LD	0	9	-4	2	0	6	-3	2
Showalter Index	CD	2	9	-2	3	2	9	-1	3
(°C)	NCD	4	13	-1	4	3	15	-1	3
	LD	45	51	33	3	45	50	38	2
Total Totals	CD	43	49	34	4	43	48	34	4
(°C)	NCD	40	47	25	5	42	47	23	5
	LD	2202	4303	306	929	2473	3934	242	663
CAPE	CD	2015	3851	88	814	1837	3293	17	800
(J kg^{-1})	NCD	1496	3041	0	1057	1614	2983	122	880
	LD	-32	0	-157	35	-18	0	-140	16
CIN	CD	-25	0	-69	21	-19	0	-55	17
(J kg^{-1})	NCD	-61	0	-213	65	-42	0	-201	55
	LD	877	974	733	55	888	971	728	45
LFC	CD	879	964	772	50	871	957	750	52
(mb)	NCD	814	1014	429	129	827	1020	0	172

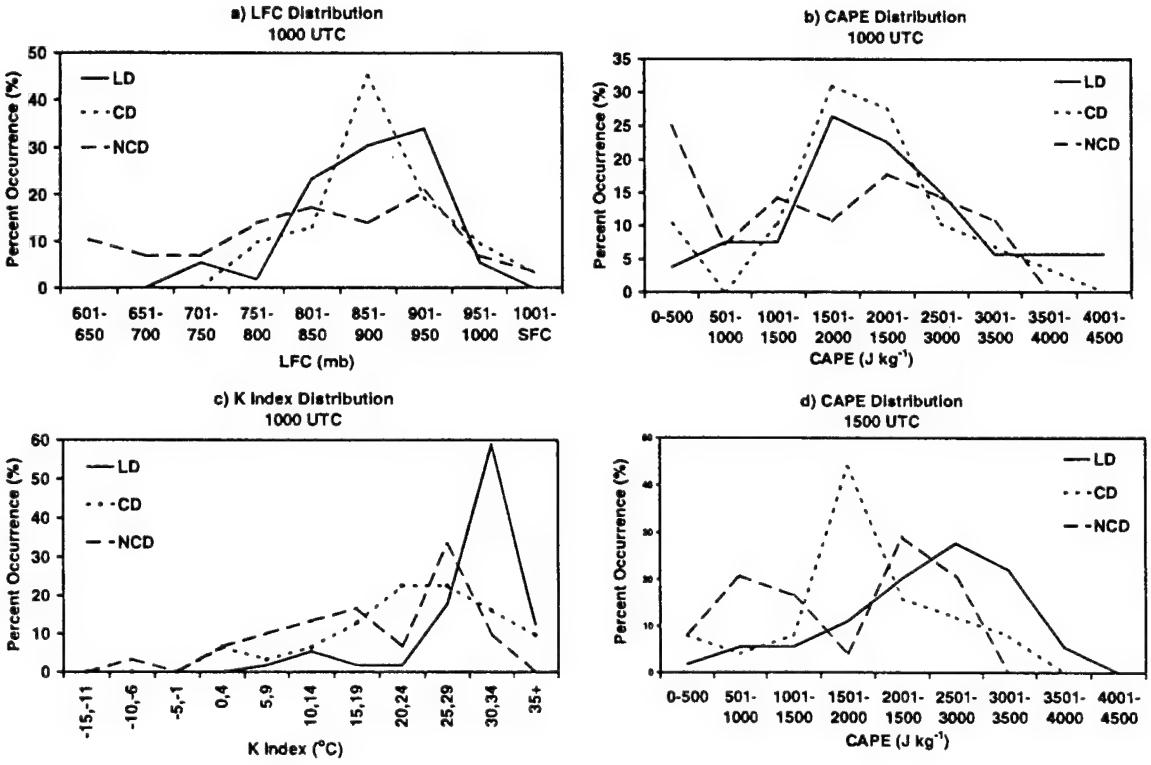

Fig. 13. Frequency distributions of a) LFC, b) CAPE, and c) K Index at 1000 UTC and d) CAPE at 1500 UTC.

Mean values of the Showalter Index, Lifted Index, Total Totals, and CAPE at 1000 UTC are different among the three convection categories (Table 4). In the mean, LD have the most unstable values, while the least stable values are for NCD. However, frequency distributions of these parameters do not exhibit distinct differences between categories. The distribution for CAPE (Fig. 13b) is representative of these indices. MRPP results show that these indices do not discriminate between LD and CD (Table 2). The Lifted Index yields the best p-value (0.200 at 1000 UTC). CAPE is the worse discriminator at 1000 UTC with a 0.98 p-value.

Mean values of the K Index at 1000 UTC exhibit the best overall differentiation between categories. Almost 60 percent of all LD have K Indices between 30 – 34°C, as compared to only 10 percent of CD and 15 percent of NCD (Fig. 13c). However, frequency differences between the CD and NCD distributions are not pronounced. Unlike the other stability parameters, the K Index does show statistically significant discrimination between the LD and CD categories at 1000 UTC with a 0.004 p-value (Table 2).

At 1500 UTC, the Showalter Index and CAPE provide good differentiation among mean values, i.e., 0, 2, and 3°C for the Showalter Index and 2473, 1837, and 1614 J kg^{-1} for CAPE (Table 4), particularly between LD and CD. The CAPE frequency distribution (Fig. 13d) (Showalter Index not shown), shows a distinct difference in the values of peak occurrence. Unfortunately, the NCD distribution is broad, with the maximum falling between the LD and CD peak values. No parameter at 1500 UTC has the statistically significant p-value of ≤ 0.05 for the LD versus CD comparison (Table 2). CAPE is closest with a 0.09 p-value.

Current results indicate that forecasters should emphasize the K Index from the 1000 UTC sounding. If the 1500 UTC sounding is available before forecast preparation, CAPE also may be helpful. Indeed, based on the TSS (Table 3) the K Index at 1000 UTC shows the best forecast skill of all parameters examined, i.e., TSS = 0.58 using a threshold of 30°C. The POD is large (0.77) while the POFD is small (0.19). These results are better than those of Fuelberg and Biggar (1994) where the K Index produced a 0.19 TSS for forecasting strong convective days versus weak or non-convective days in the Florida panhandle. It is not surprising that the K Index produces the best forecasting score. It is considered one of

the best stability parameters for forecasting thunderstorms under weak synoptic forcing (Sadowski and Reick 1977). Generally speaking, a K Index of 30°C east of the Rocky Mountains implies approximately a 40 percent probability of thunderstorms, while the range 31 to 35°C suggests a 40 to 60 percent probability of thunderstorms. Fig. 13c shows this relation almost exactly, with nearly 60 percent of LD occurring when K Indices are between 31-35°C.

c. Area-Average Divergence

Area-averaged horizontal divergence is the last parameter examined as a possible convective signature with the ECSB. Using mesonetwork winds at the 54 ft level, Watson et al. (1991) related area-averaged divergence to the probability of lightning. They found that a sustained drop of 75×10^{-6} s^{-1} (hereafter referred to as 75 units) was followed by CGL 61 percent of the time. Similarly, a drop of 100 units resulted in CGL 68 percent of the time, while a drop of 150 units resulted in CGL 82 percent of the time. This technique obviously is intended to be a nowcasting tool and, in fact, works well enough to be currently used by 45WS forecasters in that capacity (Pinder and Weems 1997, personal communication). Although Watson et al. (1991) did not categorize days as being sea breeze influenced or not, the current study focuses only on undisturbed ECSB days. We examined the usefulness of area-averaged divergence as a nowcasting tool in these particular ECSB situations. Furthermore, we investigated whether area-averaged divergence can be used as a longer range (6-12 h) forecasting tool.

Fig. 14 is a time series of composite area-averaged horizontal divergence for LD, CD, and NCD from 1000 to 2400 UTC. All categories exhibit a similar pattern of weak divergence during the early morning, followed by a sustained decrease until approximately 1730 UTC, and then an increase after approximately1930 UTC. There is strong convergence in all three categories during the afternoon, even on NCD. The greatest difference between LD and the other categories occurs between 1700 and 1900 UTC, when LD are slightly more convergent, e.g., composite LD divergence exceeds -75×10^{-6} s^{-1}, while the other categories only reach approximately -60×10^{-6} s^{-1}. At 1200 UTC, LD is more divergent than the

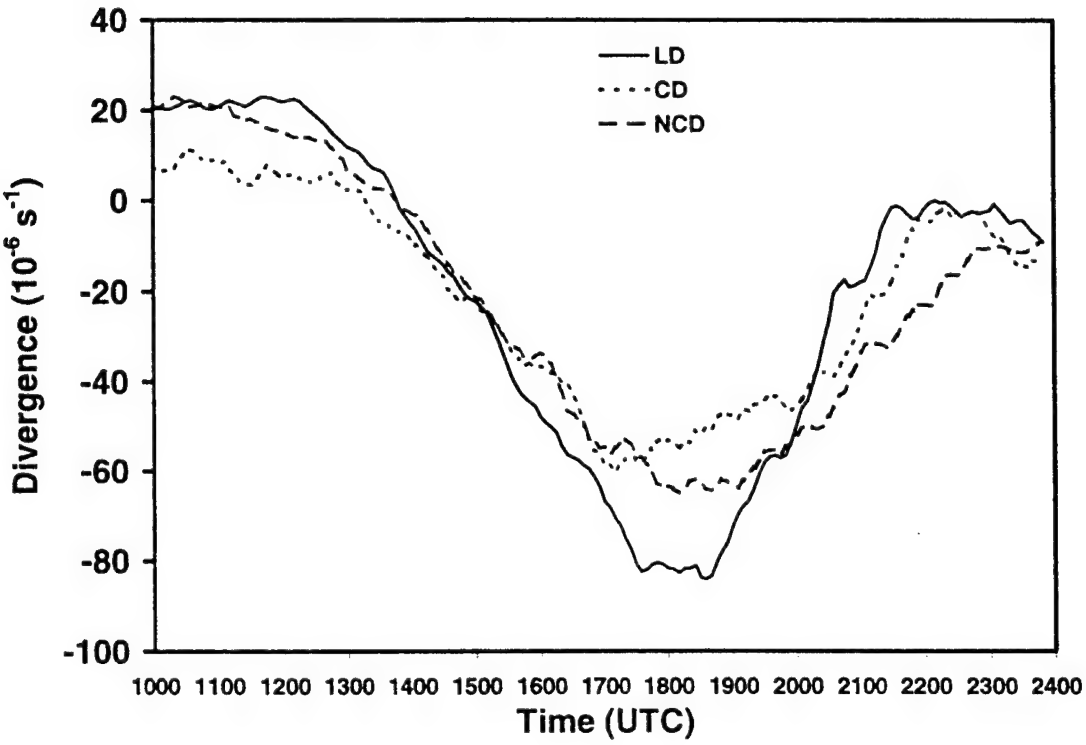

Fig. 14. Time series of composite AAD.

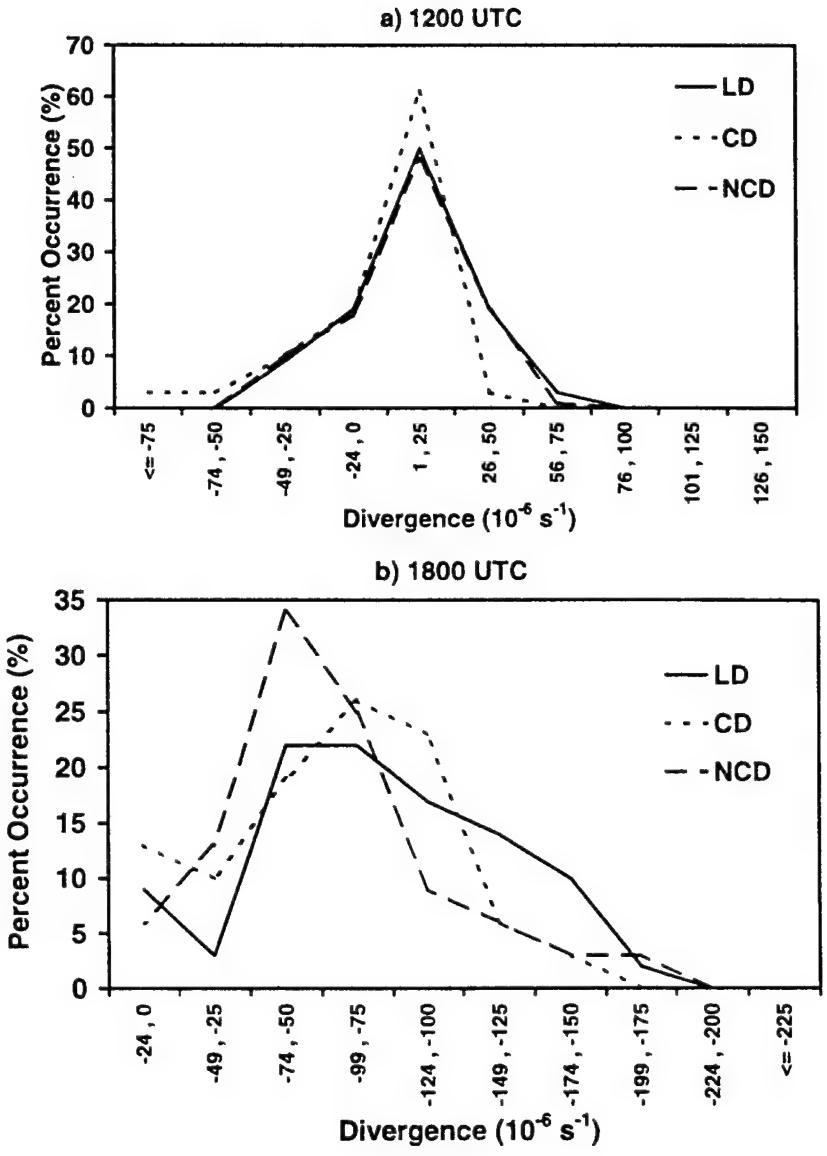

Fig. 15. Frequency distributions of AAD at a) 1200 UTC and b) 1800 UTC.

other categories. This time is examined for a possible early morning signature on which to base an afternoon convection forecast. Frequency distributions of area-averaged divergence were calculated at 1200 (Fig. 15a) and 1800 UTC (Fig. 15b). Unfortunately, little difference is indicated between the categories at 1200 UTC. LD, CD and NCD each have peak values in the range 1 to 25×10^{-6} s^{-1}. Even worse, in terms of an early convective signature, LD and NCD have nearly identical distributions. Thus, divergence at 1200 UTC appears to be of no use in distinguishing between convection categories later in the day. Although there is better differentiation at 1800 UTC (Fig. 15b) peak values still are similar, and the distributions are broad and spread across a large range.

The composite time series of AAD for all lightning days, indexed to the first lightning strike (Fig. 16), shows the evolution six hours prior to the first CGL strike and two hours after. The trend is for decreasing divergence that reaches a minimum just prior to the first strike. Although similar to the actual event shown in Fig. 5, there is no sharp drop in divergence in the composite event. This lack of a convergence signature in the composite occurs because horizontal divergence values leading up to the first strike vary significantly from day to day. In fact, on the individual days we examined, there often was not the well-defined, semi-continuous decrease in divergence shown in Fig. 5. As a result, our relations between divergence and lightning are not as good as those of Watson et al. (1991). At the 75 unit threshold our (Watson et al. 1991) probability of CGL is 53 (61) percent, at 100 units it is 63 (68) percent, and at 150 units it is 57 (82) percent.

There are two possible reasons for our reduced agreement compared to Watson et al. (1991). First, initial surface convergence may not be as well defined with ECSB initiated convection as with storms that form inland and move into the study area. Most thunderstorms do not form over the Cape but move into the Cape area from mainland Florida. Such storms often are associated with a strong combined outflow boundary/west coast sea breeze front, or simply, West Coast Front (WCF). Wilson and Megenhardt (1996) provide an excellent description of the phenomena. They show that the WCF has stronger low-level convergence than the ECSB front and that convection along the WCF is more vigorous, thereby leading to a stronger signature in the time series of area-averaged divergence, i.e., strong

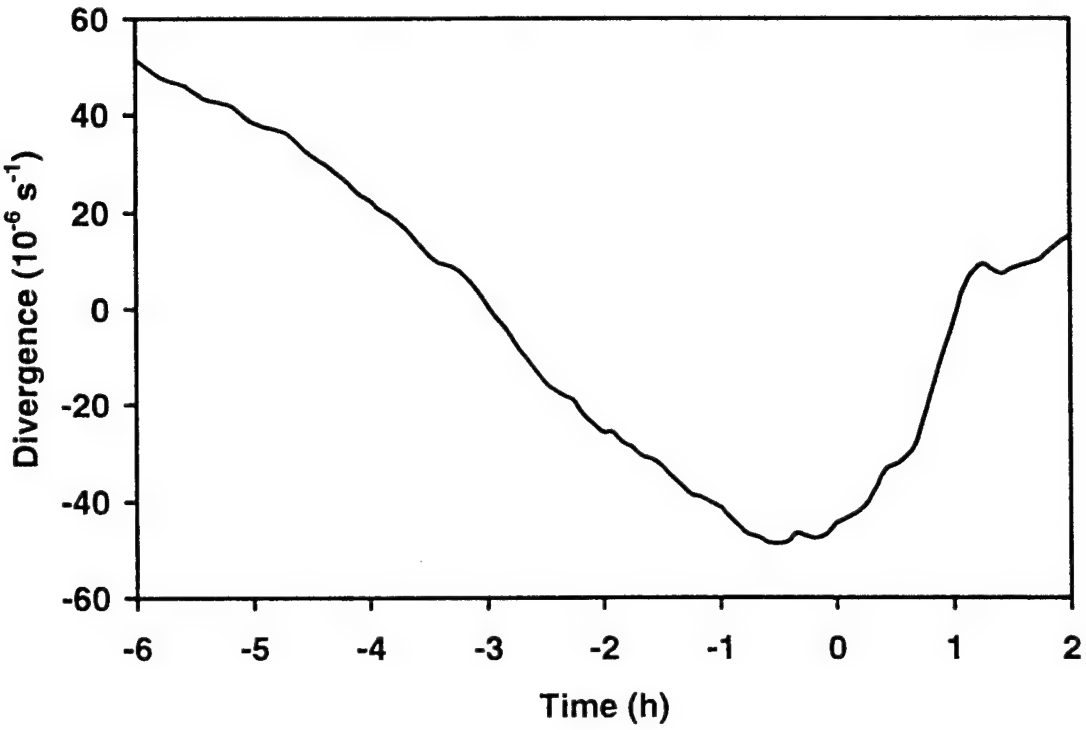

Fig. 16. AAD Times series for composite of all LD indexed to first strike. Time series starts six hours before strike and ends two hours after.

convergence. Watson et al. (1991) made no distinction as to the source of the convection in their study. Therefore, they undoubtedly had numerous events of inland convection that moved east with the WCF, whereas we removed such days from our data set.

A second possible cause is the location where the majority of ECSB storms forms. Based on radar imagery, most ECSB storms develop over the extreme northwest and extreme southwest portions of the study area (Fig. 1) where the ECSB front meets the inland portion of the IRB. Since these storms are on the very edge, or even outside of the CCAS/KSC mesonetwork, they produce poor AAD signatures, i.e., only weak convergence within the network.

We examined those days when the first CGL strike occurred within 20 km of the SLF to determine whether weaker initial ECSB convergence, or storm formation near the outer edges of the mesonetwork, cause the reduced agreement with Watson et al. 1991. Since radar imagery showed that most sea breeze related storms are no more than several tens of kilometers in diameter, any storm that develops within 20 km of the center of the mesonetwork will be contained within its boundaries. Such storms should produce the expected sharp decrease in AAD, e.g., Fig. 5. Unfortunately, there were only 14 days on which the first strike was within 20 km of the SLF. Wilson and Megenhardt (1996) showed a similar lack of thunderstorms initiated solely by the ECSB. However, all AAD time series for these 14 days did exhibit a sharp drop in divergence prior to the first lighting strike. The magnitude of these drops is similar to that reported by Watson et al. (1991). This finding indicates that our lack of a well defined signature in the divergence time series set likely is due to storms developing on the edges of the tower mesonetwork.

Current results suggest that surface area-averaged divergence is not a useful tool for forecasting ECSB thunderstorms, even in a nowcasting role. This is shown statistically by the TSS results in Table 3. A threshold of a 75 unit drop in divergence produced the best TSS, 0.15. AAD has a good POD (0.79) but in turn has a high POFD (0.64). This shows that area-averaged divergence must be used with care due to its high false alarm rate. This is a major limitation of the AAD technique.

4. SUMMARY AND CONCLUSION

This study has examined undisturbed East Coast Sea Breeze (ECSB) days near Cape Canaveral Florida. The goal was to document the characteristics of these days and to find useful indicators for thunderstorms initiated by the ECSB forcing mechanism. Convection associated with the ECSB is difficult to forecast because it forms over the Cape itself. There often is no opportunity to "see it coming".

Warm season days from 1996 and 1997 were carefully screened to ensure a complete data set of undisturbed ECSB days. We found 120 undisturbed ECSB days. These days were categorized based on convective activity along the sea breeze front, i.e., lightning days (LD), cell days (CD), and no cell days (NCD). Convective categories were compared and contrasted based on synoptic flow patterns, sea breeze type, sea breeze passage time, several stability parameters, and wind and RH profiles. Stability, wind, and RH parameters were calculated from the 1000 and 1500 UTC Cape Canaveral radiosonde sounds and tested for statistical discrimination between convection category using MRPP. Results compared LD versus CD, and LD versus a combined CD + NCD category. However, the LD versus CD comparison was the primary focus this study. The TSS was used to determine the forecasting skill of identified parameters. Area-averaged horizontal surface divergence also was examined as a tool for both short term (0-3 h) and longer term (6-12 h) forecasting.

We found that thunderstorm development on undisturbed ECSB days is most likely with southwest or southeast low-level wind flow. Thunderstorms also are more likely to occur if there is a SB1/SB2 type sea breeze. Results indicate that the occurrence of a TCL increases the likelihood of cloud to ground lightning, while the occurrence of a river breeze does not increase that likelyhood. The occurrence of both a TCL and a river breeze also does not indicate an increased risk of thunderstorms.

Statistically, the *v* wind component from the 1000 UTC radiosonde sounding is the best discriminator of LD versus CD for undisturbed ECSB days. Convective days generally have a negative, i.e., southerly, *v* wind component, while non-convective days generally show a positive *v* wind component. Conversely, the *u* wind component is poor discriminator, differing little between convective categories. The *v* wind at 850 mb exhibits even better forecast skill than the 700 mb *v* wind component.

RH did not show statistically significant differences between convective categories at either sounding time. However, the 700 mb RH was closest to showing statistically significant discrimination and showed forecasting skill comparable to that of the 850 mb *v* wind.

The 1000 UTC K Index was the only stability parameter to statistically discriminate between convective categories. It also had the best forecasting skill of the parameters tracked in this study. The CAPE and Lifted Index from 1500 UTC were other stability parameters that showed promising forecast skill.

Surface area-averaged, horizontal divergence was shown to be of little use as a forecasting tool because most ECSB initiated convection forms outside of the current CCAS/ KSC mesonetwork. Lightning producing convection initiated solely by the ECSB is rare near the center of the study area. On only 14 days (24 percent of all lightning days) of this two year study did an undisturbed ECSB cause a lightning strike within 20 km of the SLF. To adequately capture the area-averaged divergence signature for the remaining 76 percent of the lightning days, the CCAS/KSC mesonetwork must be expanded into the preferred area of storm development, i.e., the extreme northwest and southwest sections of the study area.

This research has documented characteristics of undisturbed ECSB days and found the best indicators for forecasting thunderstorm activity on the ECSB as it transits the Cape Canaveral area. Although several parameters have been shown to be useful, further research is needed to maximize their potential as forecasting tools. Better forecasting skill will result if the best parameters noted here are used to produce multiple regression equations similar to those developed by Nuemann (1971a).

REFERENCES

Arritt, R. A., 1993: Effects of the large-scale flow on characteristic features of the sea breeze. *J. Appl. Meteor.*, **32**, 116-125.

Atkins, N. T., R. M. Wakimoto and T. M. Weckwerth, 1995: Observations of the sea-breeze front during CaPE. Part II: Dual-Doppler and aircraft analysis. *Mon. Wea.Rev.*, **123**, 944-969.

Bauman, W. H., III, 1995: Synoptic and mesoscale forcing of convective activity over Cape Canaveral during easterly flow and nowcasting for Space Shuttle landings at Kennedy Space Center. Ph.D. dissertation, North Carolina State University, Raleigh, NC, 140 pp.

Bechtold, P., J. Pinty, and P. Mascart, 1991: A numerical investigation of the influence of large-scale winds on the sea-breeze-and inland-breeze-type circulations. *J. Appl. Meteor.*, **30**, 1268-1279.

Blanchard, D. O. and R. E. Lopez, 1985: Spatial patterns of convection in south Florida. *Mon. Wea. Rev.*, **113**, 1282-1298.

Burpee, R.W., 1979: Peninsula-scale convergence in the south Florida sea breeze. *Mon. Wea. Rev.*, **107**, 852-860.

Burpee, R. W., and L. N. Lahiff, 1984: Area-averaged rainfall variations on sea-breeze days in south Florida. *Mon. Wea, Rev.*, **112**, 520-534.

Byers, H. R. and H. R. Rodebush, 1948: Causes of thunderstorms of the Florida peninsula. *J. Meteor.*, **5**, 275-280.

Cetola, J. D., 1997: A climotology of the sea breeze at Cape Canaveral, Florida. M.S. thesis, Florida State University, Tallahassee, FL, 56 pp.

Cooper, H. J., M. Garstang and J. Simpson, 1982: The diurnal interaction between convection and peninsular-scale forcing over south Florida. *Mon. Wea. Rev.*, **110**, 486-503.

Doswell, C.A., III, and J. A. Flueck, 1989: Forecasting and verifying in a field research project: DOPLIGHT '87. *Wea. Forecasting*, **4**, 97-109.

Estoque, M.A., 1962: The sea breeze as a function of the prevailing synoptic situation. *J. Atmos. Sci.*, **19**, 244-250.

Frank, N. L., and D. L. Smith, 1968: On the correlation of radar echoes over Florida with various meteorological parameters. *J. Appl. Meteor.*, **7**, 712-714.

Fuelberg, H. E., and D. G. Biggar, 1994: The preconvective environment of summer thunderstorms over the Florida panhandle. *Wea. Forecasting*, **9**, 316-326.

Gentry, R. C. and P. L. Moore, 1954: Relation of local and general wind interaction near the sea coast to time and location of air-mass showers. *J. Meteor.*, **11**, 507-511.

Guillory, A. R. and G. J. Jedlovec, 1994: A mesoscale analysis of a Florida sea breeze from CaPE. Preprint, *6th Conf. on Mesoscale Processes*, Portland, Amer. Meteor. Soc., 238-241.

Harms, D. E., B. F. Boyd, R. M. Lucci, M.S. Hinson, and M. W. Maier, 1997: Systems used to evaluate the natural and triggered lightning threat to the eastern range and Kennedy Space Center. *Preprint, 28th Conference on Radar Meteorology* , Austin, TX, Amer. Meteor. Soc., 240-241.

Intrieri, J. M., et. al., 1990: The land/sea breeze experiment (LASBEX). *Bull. Amer. Meteor. Soc.*, **71**, 656-664.

Jehn, K. H., 1973: A sea breeze bibliography, 1664-1972. Report No. 37, Atmospheric Sciences Group, University of Texas at Austin, Austin, TX, 51 pp.

Kingsmill, D. E., 1995: Convection initiation associated with a sea-breeze front, a gust front, and their collision. *Mon. Wea. Rev.*, **123**, 2913-2933.

Laird, N. F., D. A. R. Kristovich, H. T. Ochs III and R. M. Rauber, 1994: Mesoscale Interactions within the boundary layer behind the Cape Canaveral sea-breeze front. Preprint, *6th Conf. on Mesoscale Processes*, Portland, Amer. Meteor. Soc., 284-287.

Laird, N. F., D. A. R. Kristovich, H. T. Ochs III, R. M. Rauber and L. J. Miller, 1995: The Cape Canaveral sea and river breezes: Kinematic structure and convective initiation. *Mon. Wea. Rev.*, **123**, 2942-2956.

Lopez, R. E., P. T. Gannon, Sr., D. O. Blanchard and C. C. Balch, 1984: Synoptic and regional circulation parameters associated with the degree of convective shower activity in south Florida. *Mon. Wea. Rev.*, **112**, 686-703.

Lopez, R. E. and R. L. Holle, 1987a: The distribution of summertime lightning as a function of low-level wind flow in Central Florida. *NOAA Technical Memorandum ERL ESG-28.*

Lopez, R E. and R L. Holle, 1987b: A study of the interaction between the sea breeze and the synoptic flow using lightning data. Preprint, *17th Conf. on Hurricanes and Tropical Meteorology*, Miami, Amer. Meteor. Soc., 82-85.

Lyons, W.A., 1972: The climatology and prediction of the Chicago Lake Breeze. *J. Appl. Meteor.*, **11**, 1259-1270.

Lyons, W. A., C. J. Tremback, R. L. Walko, M. E. Nicholls, I. Baker, W. Thorson, R. A. Pielke and W. R. Cotton, 1995: Towards operational thunderstorm forecasting at the Kennedy Space Center using the parallelized version of RAMS on a workstation cluster. Preprint, *14th Conf. on Weather and Forecasting*, Dallas, Amer. Meteor. Soc., 471-474.

Manobianco, J., J. W. Zack, and G. E. Taylor, 1996: Workstation-based real-time mesocasle modeling designed for weather support to operations at the Kennedy Space Center and Cape Canaveral Air Station. *Bull. Amer. Meteor. Soc.*, **77**, 653-671.

McPherson, R. D., 1970: A numerical study of the effect of a coast irregularity on the sea breeze. *J. Appl. Meteor.*, **9**, 767-777.

Mielke, P. W., K. J. Berry, and E. S. Johnson, 1976: Multi-response permutation procedures for *a priori* classifications. *Commun. Statist. Theor. Meth.*, **A5**, 1409-1424.

Mielke, P. W., K. J. Berry, and G. W. Brier, 1981: Applications of multi-response permutation procedures for examining seasonal changes in monthly mean sea-level pressure patterns. *Mon. Wea Rev.*, **109**, 120-126.

Neumann, C. J., 1970: Frequency and duration of thunderstorms at Cape Kennedy part II. *ESSA Technical Memorandum WBTM SOS-6.*

Neumann, C. J., 1971a: Thunderstorm forecasting at Cape Kennedy, Florida, utilizing multiple regression techniques. *NOAA Technical Memorandum NWS SOS-8.*

Neumann, C. J., 1971b: The thunderstorm forecasting system at the Kennedy Space Center. *J. Appl. Meteor.*, **10**, 921-936.

Neumann, J., 1951: Land breezes and nocturnal thunderstorms. *J. Meteor.*, **8**, 60-67.

Neumann, J., 1977: On the rotation rate of the direction of sea and land breezes. *J. Atmos. Sci.*, **34**, 1913-1917.

Nicholls, M. E., R. A. Pielke and W. R. Cotton, 1991: A two-dimensional numerical investigation of the interaction between sea breezes and deep convection over the Florida peninsula. *Mon. Wea. Rev.*, **119**, 298-323.

Pielke, R. A., 1974: A three-dimensional numerical model of the sea breezes over South Florida. *Mon. Wea. Rev.*, **102**, 115-139.

Pielke, R. A., 1984: *Mesoscale Meteorology Modeling.* Academic Press, 612 pp.

Reed, J. W., 1979: Cape Canaveral sea breezes. *J. Appl. Meteor.*, **18**, 231-235.

Sadowski, A. F., and R. E. Rieck, 1977: Technical Procedures Bulletin No. 207: Stability indices. National Weather Service, Silver Spring, MD, 8 pp.

Simpson, J.E., D.A. Mansfield, and J.R. Milford, 1977: Inland Penetration of sea-breeze fronts. *Quart. J. R. Met. Soc.*, **103**, 47-76.

Simpson, J. E., 1987: *Gravity Currents: In the Environment and the Laboratory.* John Wiley & Sons, 244 pp.

Simpson, J.E., 1994: *Sea breeze and local winds.* Cambridge University Press, 234 pp.

Taylor, G. E., M. K. Atchison and C. R. Parks, 1990: *The Kennedy Space Center Atmospheric Boundary Layer Experiment (KABLE) Phase II, Final Report*, National Aeronautics and Space Administration (NASA), Kennedy Space Center (KSC), ENSCO, Inc., 445 Pineda Court, Melbourne, FL 32940.

Ulanski, S. L., and M. Garstang, 1978: The role of surface divergence and vorticity in the life cycle of convective rainfall. Part I: Observation and analysis. *J. Atmos.Sci.*, **35**, 1047-1063.

Wakimoto, R. M. and N. T. Atkins, 1994: Observations of the sea-breeze front during CaPE. Part I: Single-Doppler, Satellite, and Cloud Photogrammetry Analysis. *Mon. Wea. Rev.*, **122**, 1092-1114.

Walsh, J. E., 1974: Sea breeze theory and applications. *J. Atmos.Sci.*, **31**, 2012-2026.

Watson, A. I., R. L. Holle, R. E. Lopez, R. Ortiz and J. R. Nicholson, 1991: Surface wind convergence as a short-term predictor of cloud-to-ground lightning at Kennedy Space Center. *Wea. Forecasting*, **6**, 49-64.

Wilson, J. W., and D. L. Megenhardt, 1997: Thunderstorm intiation, organization, and lifetime associated with Florida boundary layer convergence lines. *Mon. Wea. Rev.*, **125**, 1507-1525.

Woodley, W. L., and R. I. Sax, 1976: The Florida Area Cumulus Experiment: Rational, design, procedures, results and future course. NOAA tech. Rep. ERL 354, WMPO-6, 204 pp.

Xian, Z. and R. A. Pielke, 1991: The effects of width of landmasses on the development of sea breezes. *J. Appl. Meteor.*, **30**, 1280-1304.

Zhong, S. and E. S. Takle, 1992: An observational study of sea- and land-breeze circulation in an area of complex coastal heating. *J. Appl. Meteor.*, **31**, 1426-1438.

Zhong, S. and E. S. Takle, 1993: The effects of large-scale winds on the sea-land-breeze circulations in an area of complex coastal heating. *J. Appl. Meteor.*, **32**, 1181-1195.

Zhong, S., J. M. Leone, Jr. and E. S. Takle, 1991: Interaction of the sea breeze with a river breeze in an area of complex coastal heating. *Bound.-Layer Meteor.*, 101-139.

BIOGRAPHICAL SKETCH

Jonathan Lee Kelly was born on 30 December 1967 in New Bern, North Carolina. He graduated from West Craven High School in Craven County, North Carolina in June 1986. He received a Bachelor of Science degree in Applied Physics from East Carolina University in July 1990. At that time he was commissioned a 2nd Lieutenant in the United States Air Force. In April 1991 he was assigned to the Air Force Institute of Technology's Basic Meteorology Program at Florida State University. He completed the program in April 1992 and was assigned to Cannon Air Force Base, Clovis, New Mexico as a weather officer for the 27th Fighter Wing. He was transferred to Hanscom Air Force base in 1994 where he worked as a staff meteorologist for the Electronic Systems Center. In August 1996 Captain Kelly returned to the Air Force Institute of Technology and Florida State University to pursue a Master's Degree in Meteorology. This thesis is the culmination of that pursuit.